A FINITE ELEMENT ANALYSIS FOR PROBLEMS OF LARGE STRAIN AND LARGE DISPLACEMENT

by

AMIN SALEH ALY, B.S., M.S.

DISSERTATION

Presented to the Faculty of the Graduate School of

The University of Texas at Austin

in Partial Fulfillment

of the Requirements

for the Degree of

DOCTOR OF PHILOSOPHY

THE UNIVERSITY OF TEXAS AT AUSTIN

May, 1981

A C K N O W L E D G M E N T S

The author wishes to express his sincere appreciation to his supervising professor, Dr. Eric B. Becker, for his great experienced advice and encouragement.

The author also expresses deep thanks to the members of the Supervisory Committee, Dr. L. Hayes, Dr. J. T. Oden, Dr. M. Stern, and Dr. C. H. Yew, for their valuable comments.

A. S. A.

The University of Texas at Austin
March 22, 1981

To my wife, Fadia,

and my daughters,

Hanan and Safinaz

A FINITE ELEMENT ANALYSIS FOR PROBLEMS OF LARGE STRAIN AND LARGE DISPLACEMENT

APPROVED BY SUPERVISORY COMMITTEE

Eric B. Becker

Morris Stern

Linda J. Hayes

Chung H. Yew

J. Tinsley Oden

C H A P T E R I

INTRODUCTION

1.1 General

This work is concerned with the development of a general finite element formulation method for problems with large strains and large displacements of nonlinear isotropic hyperelastic rubber-like materials. A numerical method for treating such nonlinear elasticity problems can be found in the fundamental treatment given by Becker [3]. More complete description was given by Oden [20]. Here we review some relatively recent work in this area.

1.2 Historical Review

Concerning the application of finite element methods to the solution of problems on rubber-like materials, we note that there are basically two categories of analysis. In the first category, the material is treated as nearly incompressible and uses finite element models in which displacement is the only variable. In the second category, the material is treated as incompressible, and

mixed finite element models, in which both displacement and hydrostatic pressure are used. The mixed models are more popular in the literature, and were implemented in finite element formulation methods before the displacement models.

1.2.1 Mixed Models

This category is sometimes referred to as multiplier methods. The available mixed formulation methods, for rubber-like materials, may be summarized as follows:

1.2.1.1 Oden and Key's Method. In 1970, Oden and Key [21] developed an incremental solution based on the minimum potential energy principle. They used a constant strain triangular element with both the nodal displacement and constant hydrostatic pressure as variables. The method was applied for the solution of many interesting problems. One of these problems, for which we have included many results, was for a thick pressurized cylinder of Mooney material. The accuracy of the solution of this problem depended on the number of load increments, since the governing equations were linearized at each load increment and no iterative corrections were made.

1.2.1.2 Scharnhorst and Pian's Method. In 1978, Scharnhorst and Pian [27] developed an incremental solution, based on a Reissner [7] type variational principle. In this approach, three fields are separately discretized: the displacement, the hydrostatic pressure and the distortional stress. The discretization parameters for the latter field were eliminated at the element levels. They used a four-node isoparametric element with constant pressure for the solution of the pressurized cylinder solved by Oden and Key. Here also, because the method is strictly incremental, the accuracy of the resulting solution depends on the number of load increments used.

1.2.1.3 R. C. Batra's Method. In 1980, Batra [2] followed Oden's method. He used a four-node element with both the displacement and constant hydrostatic pressure as variables, and reconsidered the pressurized cylinder mentioned before. The accuracy and efficiency of the resulting solutions were compared in the presence and absence of equilibrium iterations in the incremental formulation. The accuracy of the solution depended on the number of load increments and the number of iterations allowed for each load increment.

1.2.1.4 Oden and Le Tallec's Method. During the course of this study, Oden and Le Tallec [13, 23]

developed an Augmented Lagrangian formulation for Mooney and neo-Hookean materials. The equilibrium equations obtained were solved using an external Uzawa algorithm, which is associated with a fixed, positive definite matrix. Certain transformations must be performed, depending on the nonlinearity in the energy form used, so that the resulting matrix be constant. In this sense, the method may not be as general as Newton's method which treats the various types of nonlinearity with the same ease. On the other hand, the Uzawa technique was shown to be very powerful. One of the applications was for a compression of a thick beam fixed at both ends. Two solutions could be obtained in the same computer run, a result that may not be possible to get using Newton's method.

1.2.2 Displacement Models

This category is also referred to as the penalty methods. The displacement formulation methods, which have been reported for rubber-like materials may be summarized as follows.

1.2.2.1 Skala's Method. In 1975, Skala [28] developed a finite element formulation method, based on

the minimum potential energy principle, for the analysis of compressible neo-Hookean materials. An eight-node isoparametric element was used. The nonlinear equilibrium equations were solved by Newton's method. He found that complete formulation of the entire stiffness matrix at every iteration is more efficient than several other alternatives. The method was used [29] for the solution of a pressurized cylinder similar to the problems considered by Oden and Key, but with different data. The author noticed "some oscillation in the calculated stresses as the material becomes more incompressible." The present work is, in some sense, an extension of the work of Skala.

1.2.2.2 Cescotto and Fonder's Method. In 1979, Cescotto and Fonder [6] extended Nagtegaal's principle [7] to the domain of nonlinear elasticity for hyperelastic materials. They followed lines similar to those used by Oden and Key, in the case of incompressible materials. They obtained an exact expression for the incremental second Piola Kirchoff stress in terms of the increment of Green's strain. The method was applied for the solution of a hollow sphere. Concentric spherical elements were used. The solution obtained matched the exact solution derived by Green and Zerna [8].

1.2.2.3 Malkus and Hughes' Method. Malkus and Hughes [16] developed a displacement method that mimics a certain class of mixed methods, and employs reduced/selective integration techniques. The method was applied by Malkus [17] for the stretching of a tensile test specimen of dogbone-shaped rubber sheet of Mooney material. Solutions were obtained by considering the problem both as a plane stress and three-dimensional body. The three-dimensional solution was sensitive to the penalty parameter as well as the mesh size.

1.2.2.4 Jankovich et al.'s Method. Jankovich et al. [12] developed a displacement method that uses a "reduced constraint concept." The method is similar to that of Malkus [16], but does not use reduced integration which, according to [12], "may lead to instabilities when the current iteration displacement vector is far from solution and/or the FEL grid is too coarse." Two problems were solved using a Rivlin constitutive law of the form

$$U(I_1, I_2) = \sum_{i+j=1}^{3} c_{ij}(I_1 - 3)(I_2 - 3)$$

which has nine coefficients.

The first problem was for the extension of an axisymmetric body under central point load. The second problem was for a hollow cylinder subjected to imposed radial displacement on its inside wall. The computer results showed good agreement with both analytical and experimental results.

1.2.3 Comments

In evaluating the work mentioned above, the following comments can be made:

1. It is not clear, from previous work, which of the two formulations (mixed and penalty) is to be preferred. Indeed all materials are at least slightly compressible--the idea of incompressibility was introduced only to simplify the mathematical model. Whether or not computational methods are made easier by this assumption is another question--one that this work may help answer.
2. Previous work does not include a thorough treatment of changing in loading due to deformations, i.e., load stiffness, which can be essential for the class of problems under consideration.

3. The previous works are limited to the use of specific forms of constitutive laws, which may not be appropriate to model a particular rubber-like material at all strain levels. Indeed Ref. [12] uses a fairly complicated constitutive law, but switching from this form to another complicated form may not be easy.

1.3 Thesis Objectives

The following items were considered as primary criteria in the present work:

1. The formulation should be based on a sound theoretical basis.
2. Accommodate a variety of constitutive laws.
3. Treat cases when loading changes due to deformations.
4. Use both mixed and displacement models.

1.4 Thesis Presentation

The thesis is divided into five chapters. In Chapter II we give an abstract analysis for the problem of a body of hyperelastic isotropic material, with

strain energy expressed as a function of three strain invariants. The body is subjected to both body and traction forces. For the mathematical description of the problem, the principle of virtual work is applied. Sources of nonlinearity are investigated, then the Newton-Raphson method is applied to solve the resulting nonlinear equations. Quadratic finite elements are used. Of particular interest is a quadrilateral element in which the pressure is discretized using a linear interpolation, so the pressure is not conforming along element boundaries. This element was suggested by Professor Oden, and is shown to behave as well as the corresponding quadrilateral element with conforming pressure. However the nonconforming pressure element is more efficient.

In Chapter III we formulate the finite element matrices appearing in the rate form of the virtual work statement. The calculations are divided into two parts. The first part deals with the internal virtual work which produces the tangent stiffness matrix. The second part deals with the external virtual work, which may result in load stiffness matrices.

Chapter IV describes computed results for two problems. The first problem is a pressurized plane

strain thick cylinder. The solution is obtained using different types of elements, different integration rules, and differing grids. Our solution is compared to some solutions obtained by other investigators; also we compared between the results using both the mixed and displacement models.

The second problem is compression of a nonuniform prismatic block. Mainly two constitutive laws were considered. The first is a Mooney form, and the second is a Three-term form. The latter is reported in [1, 22]. Our solution is compared to some experimental test results made at the Jet Propulsion Laboratory, of the California Institute of Technology. Also, the results obtained using the mixed and displacement models are compared.

Chapter V gives summary of results and suggests further research topics.

C H A P T E R I I

ANALYSIS OF AN ABSTRACT PROBLEM

2.1 Problem Statement

We seek to determine the motion [11] of a body (Ω), Fig. (2.1), of hyperelastic isotropic material subjected to

1. Body force ($\underset{\sim}{f}$) per unit mass.
2. Surface traction ($\underset{\sim}{t}$) per unit area of the boundary ($\partial\Omega_2$) on which the traction force acts.
3. Imposed displacement on ($\partial\Omega_1$) such that

$$\underset{\sim}{u} = \underset{\sim}{u}_0 \text{ on } (\partial\Omega_1) \tag{2.1}$$

where

$$\partial\Omega_1 \cup \partial\Omega_2 = \partial\Omega$$

$$\partial\Omega_1 \cap \partial\Omega_2 = \emptyset \ .$$

The body is expected to undergo large strains. Before we present the mathematical description of the

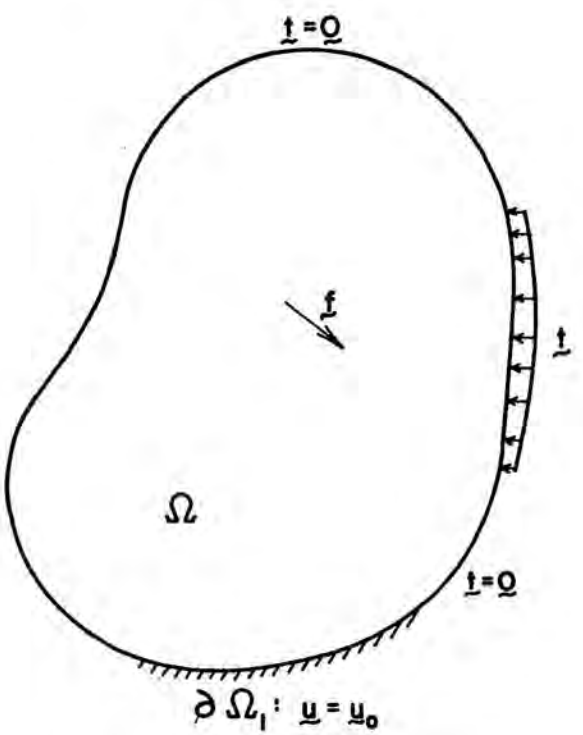

Fig. (2.1). Problem Description

problem, a review of some basic finite elasticity equations is given. More details can be found in [8] and [30].

2.1.1 Basic Equations of Finite Elasticity

Consider a homogeneous isotropic elastic body, in its undeformed state.

Let

x_k be the coordinates of a typical point of the undeformed body in a fixed cartesian coordinate system (x);

ζ^k be the coordinates of this point in an arbitrary curvilinear coordinate system (ζ) which is fixed in the body and deforms with it;

X_k be the coordinates of the same point of the deformed body in system (x);

$\underset{\sim}{i}_k$ be a cartesian base vector.

The indices take the values 1, 2 and 3, and repeated indices will mean summation, unless otherwise stated.

The covariant base vectors of the system (ζ) in the undeformed and deformed body are

$$\underset{\sim}{g}_k = \frac{\partial \underset{\sim}{x}}{\partial \zeta^k} \tag{2.2}$$

$$\underset{\sim}{G}_k = \frac{\partial \underset{\sim}{X}}{\partial \zeta^k} \tag{2.3}$$

respectively, where

$\underset{\sim}{x}$, $\underset{\sim}{X}$ are the position vectors from the origin of the system (x) to a typical point, in the undeformed states, respectively.

The displacement vector ($\underset{\sim}{u}$) is given by

$$\underset{\sim}{u} = \underset{\sim}{X} - \underset{\sim}{x} \ . \tag{2.4}$$

The squares of the line elements in the undeformed and deformed body are given by

$$ds^2 = d\underset{\sim}{x} \cdot d\underset{\sim}{x} = g_{ij} \, d\zeta^i \, d\zeta^j \tag{2.5}$$

$$dS^2 = d\underset{\sim}{X} \cdot d\underset{\sim}{X} = G_{ij} \, d\zeta^i \, d\zeta^j \ , \tag{2.6}$$

respectively, where

$$g_{ij} = \mathbf{g}_i \cdot \mathbf{g}_j \tag{2.7}$$

$$G_{ij} = \underset{\sim}{G}_i \cdot \underset{\sim}{G}_j \tag{2.8}$$

and g_{ij}, G_{ij} are the covariant components of the metric tensors of the system (ζ) in the undeformed and deformed body, respectively. The corresponding contravarient components are given by

$$g^{ij} = (1/g)c^{ij}, \qquad g = |g| \tag{2.9}$$

$$G^{ij} = (1/G)C^{ij}, \qquad G = |G| \tag{2.10}$$

where

c^{ij} is the cofactor of g_{ij} in the determinant $|g|$ of $\underset{\approx}{g}$.

C^{ij} is the cofactor of G_{ij} in the determinant $|G|$ of $\underset{\approx}{G}$.

The equilibrium equations in the deformed configuration are governed by:

$$\tau^{ij}|_i + \rho f_j = 0. \tag{2.11}$$

The stroke represents covariant differentation, and

ρ is the mass density.

τ^{ij} are the contravariant components of the stress tensor (referred to the convected coordinate system $\underset{\sim}{G}_j$),

f_j are the components of the body force density per unit mass (referred to $\underset{\sim}{G}_j$).

If the traction $\underset{\sim}{t} = t^j \underset{\sim}{G}_j$ acts on the portion $(\partial\Omega_2)$ of the surface of the body and if $\underset{\sim}{n} = n_i \underset{\sim}{G}^i$ is the unit normal to the surface then the boundary values of the tractions are given by the equations exhibited below

$$t^j = \tau^{ij} n_i \qquad \text{on } (\partial\Omega_2) \,. \tag{2.12}$$

The strain energy (U), for a compressible homogeneous elastic isotropic solid, is a function of three strain invariants, I_1, I_2 and I_3. The invariants are given by

$$I_1 = g^{ij} G_{ij} \tag{2.13}$$

$$I_2 = g_{ij}\, G^{ij}\, I_3 \tag{2.14}$$

$$I_3 = \frac{G}{g} \quad . \tag{2.15}$$

The stress ($\underset{\sim}{\tau}$) is given in terms of both the strain energy (U) and the metric tensors, by the following equation:

$$\tau^{ij} = \phi\, g^{ij} + \psi\, B^{ij} + P\, G^{ij} \tag{2.16}$$

where

$$\phi = \frac{2}{\sqrt{I_3}} \frac{\partial U}{\partial I_1} \tag{2.17}$$

$$\psi = \frac{2}{\sqrt{I_3}} \frac{\partial U}{\partial I_2} \tag{2.18}$$

$$P = 2\sqrt{I_3}\, \frac{\partial U}{\partial I_3} \tag{2.19}$$

$$B^{ij} = I_1 g^{ij} - g^{ir}\, g^{js}\, G_{rs} \quad . \tag{2.20}$$

For incompressible materials we have

$$I_3 = 1 \tag{2.21}$$

and the strain energy U is a function of only two strain invariants (I_1, I_2). In this case, P in (2.16) will be an unspecified function whose value is consistent with equations (2.11) and (2.12).

2.1.2 The Mathematical Description of the Problem

In dealing with problems with large strains and/or large displacements, there are two approaches commonly used: Lagrangian and Eulerian [9, 18, 31, 33]. In the Lagrangian approach, all the kinematic and static variables are referred to as reference configuration of the body. If they are referred to the original (undeformed) configuration, the approach is called Total Lagrangian [9] and if they referred to the recently computed configuration, the approach is called Updated Lagrangian. The Total Lagrangian approach is adopted in this work, and is simply called the Lagrangian approach.

The mathematical problem for both the displacement and mixed models is expressed by the virtual work (=equilibrium) equations. The equivalence between the variational formulation (the first variation of the total potential energy) and the classical solutions of

boundary value problems expressed by equations (2.1), (2.11) and (2.12) for such class of materials can be found in [3].

2.1.2.1 The Displacement Model. This model is used for compressible (or nearly incompressible through the use of a penalty function) materials. In this case the only unknown is the displacement ($\underset{\sim}{u}$). The determination of ($\underset{\sim}{u}$) requires the solution of the following virtual work equation:

$$[PVW] = \delta \int_{\Omega_0} U \, dv_0 - \int_{\Omega_0} \rho_0 \underset{\sim}{f} \cdot \delta \underset{\sim}{u} \, dv_0 - \int_{\partial\Omega_2} \underset{\sim}{t} \cdot \delta \underset{\sim}{u} \, dS = 0. \tag{2.22}$$

where

dv_0 is the volume increment of the undeformed configuration of the body (Ω_0).

dS is the area increment of the deformed portion of the boundary ($\partial\Omega_2$) on which the traction ($\underset{\sim}{t}$) acts.

U is the strain energy density per unit volume of the undeformed body, given as a function of three strain invariants.

ρ_o is the mass density so that ($\rho_o dv_o$ = constant = $\rho\, dv$).

$\underset{\sim}{f}$ is the body force density per unit mass.

$\delta\underset{\sim}{u}$ is a virtual displacement consistent with the kinematic constraint on ($\partial\Omega_1$).

2.1.2.2 The Mixed Model. This model is used for incompressible materials. The incompressibility condition (2.21) is imposed by means of the Lagrange multiplier method. The multiplier (λ or p) represents extra unknown variable beside the displacement. The determination of the pair ($\underset{\sim}{u}$, λ) requires the solution of the following virtual work equation

$$[PVW]^M = \delta\int_{\Omega_0} (U + \lambda h)\, dv_o - \int_{\Omega_0} \rho_o \underset{\sim}{f}\cdot\delta\underset{\sim}{u}\, dv_o - \int_{\partial\Omega_2} \underset{\sim}{t}\cdot\delta\underset{\sim}{u}\, dS$$

$$= 0 \,. \qquad (2.23)$$

where

$U = U(I_1, I_2)$

$h = h(I_3)$

$h = 0$ is the constraint equation.

λ is the Lagrange multiplier. It is a pressure-like variable, whose interpretation for a given

strain energy (U) depends on the form of $h(I_3)$ used.

$[PVW]^M$ means virtual work statement for the mixed model.

Equations (2.22) and (2.23) are highly nonlinear with the nonlinearity being introduced through

1. kinematics of the motion: since $\underset{\sim}{f}, \underset{\sim}{t}$ and $(\partial\Omega_2)$ depend in general on the motion of the body, which is not known in advance.
2. constitutive properties of the material used; the strain energy (U) is given as a function of three strain invariants (I_k) or two for incompressible material. The invariants depend on the displacement ($\underset{\sim}{u}$); so that in the displacement model, for example, we have

$$\delta U = \frac{\partial U}{\partial I_k} \frac{\partial I_k}{\partial u_\alpha} \delta u_\alpha \, . \qquad (2.24)$$

Both $\frac{\partial U}{\partial I_k}$ and $\frac{\partial I_k}{\partial u_\alpha}$ may depend on the motion of the body. Moreover the strain

energy U and the constraint equation (2.21) are not simply quadratic forms in the displacement gradients $\nabla\underset{\sim}{u}$. A simple constitutive law (Mooney) which is a linear function of the strain invariants is, for example, a complete fourth degree polynomial in the components of $(\nabla\underset{\sim}{u})$.

2.2 Incremental Loading-- Newton's Iteration

Solution of the nonlinear equilibrium equations (2.22) or (2.23) is accomplished using Newton's method. This method consists of a linearization of the virtual work statement (PVW=0), around a known state $(\overline{\underset{\sim}{X}})$, for the displacement model, or $(\overline{\underset{\sim}{X}},\overline{\underset{\sim}{\lambda}})$, for the mixed model. Assuming [PVW] to be differentiable (Frechet), then [PVW], of the displacement model as an example, admits to an expansion of the following form

$$[\mathrm{PVW}](\overline{\underset{\sim}{X}} + d\underset{\sim}{u}) = [\mathrm{PVW}](\overline{\underset{\sim}{X}}) + D[\mathrm{PVW}](\overline{\underset{\sim}{X}})\cdot d\underset{\sim}{u} + R_{\varepsilon}(\overline{\underset{\sim}{X}}) \tag{2.25}$$

where $d\underset{\sim}{u}$ is increment in the independent variable $(\underset{\sim}{X})$, or in the variable $(\underset{\sim}{u})$, since

$$\underset{\sim}{u} = \underset{\sim}{X} - \underset{\sim}{x}$$

and R_ε is a remainder term of order $o(\|d\underset{\sim}{u}\|)$ where $\|d\underset{\sim}{u}\|$ is an appropriate norm on the increments. We shall not elaborate on these technical details. The directional derivative in (2.25) is defined by

$$D[PVW](\overline{\underset{\sim}{X}})\cdot d\underset{\sim}{u} = \lim_{\varepsilon\to 0} \frac{[PVW](\overline{\underset{\sim}{X}} + \varepsilon d\underset{\sim}{u}) - [PVW](\overline{\underset{\sim}{X}})}{\varepsilon} \quad (2.26)$$

and we will set

$$d[PVW](\overline{\underset{\sim}{X}}) = D[PVW](\overline{\underset{\sim}{X}})\cdot d\underset{\sim}{u} \ . \quad (2.27)$$

The linearization (L) of [PVW] at $(\overline{\underset{\sim}{X}})$ is given by

$$L\{[PVW](\overline{\underset{\sim}{X}})\} = [PVW](\overline{\underset{\sim}{X}}) + d[PVW](\overline{\underset{\sim}{X}}). \quad (2.28)$$

The linearized equation,

$$L = 0, \quad (2.29)$$

follows from the requirement of current equilibrium of the

body. In the present method, the linearization is applied successively within a sequence of load steps, and iternatively tries to reduce R_ε to a specified convergence tolerance. More details can be found in [20]. Upon introduction of the finite element discretization the term d[PVW] will produce a tangent matrix $[\underset{\sim}{K}_T]$, and possibly a load matrix $[\underset{\sim}{K}_L]$. The details are given in the following chapter. Here we briefly review the finite element discretization, and state the different types of elements used in the present work, for both the displacement and mixed models.

2.3 Finite Element Discretization

In finite element analysis, the domain (Ω) is partitioned into elements (Ω^e) such that

$$\Omega = \cup \Omega^e \tag{2.30a}$$

and in the two-dimensional case

$$\Omega^{ei} \cap \Omega^{ej} = \begin{cases} \emptyset \text{ (empty)} \\ \text{or} \\ \text{common vertex} \\ \text{or} \\ \text{common side} \end{cases} \tag{2.30b}$$

where

$\cup$, $\cap$ are the usual union and intersection symbols, respectively.

As the loads are applied, the body deforms so that its elements attain different configurations. We employ isoparametric elements, for which we like to think of the elements in the undeformed and deformed configurations of the body as images (maps) of a master element [4]. The shape functions, $N^i(\zeta)$, are used to establish the maps between the local coordinates (ζ) of the master element and the global coordinates (x) and (X) of the undeformed and deformed elements, as

$$\underset{\sim}{x} = \underset{\sim}{x}(\zeta) = \sum_{i=1}^{NODE} N^i(\zeta)\underset{\sim}{x}_i \qquad (2.31)$$

$$\underset{\sim}{X} = \underset{\sim}{X}(\zeta) = \sum_{i=1}^{NODE} N^i(\zeta)\underset{\sim}{X}_i \ , \qquad (2.32)$$

respectively. In (2.31) and (2.32) $\underset{\sim}{x}_i$ and $\underset{\sim}{X}_i$ are the coordinates of the (NODE) nodal points of (Ω^e) in the undeformed and deformed configurations with respect to the fixed spatial coordinate system (x). Fig. (2.2) shows a quadrilateral element in its undeformed and deformed

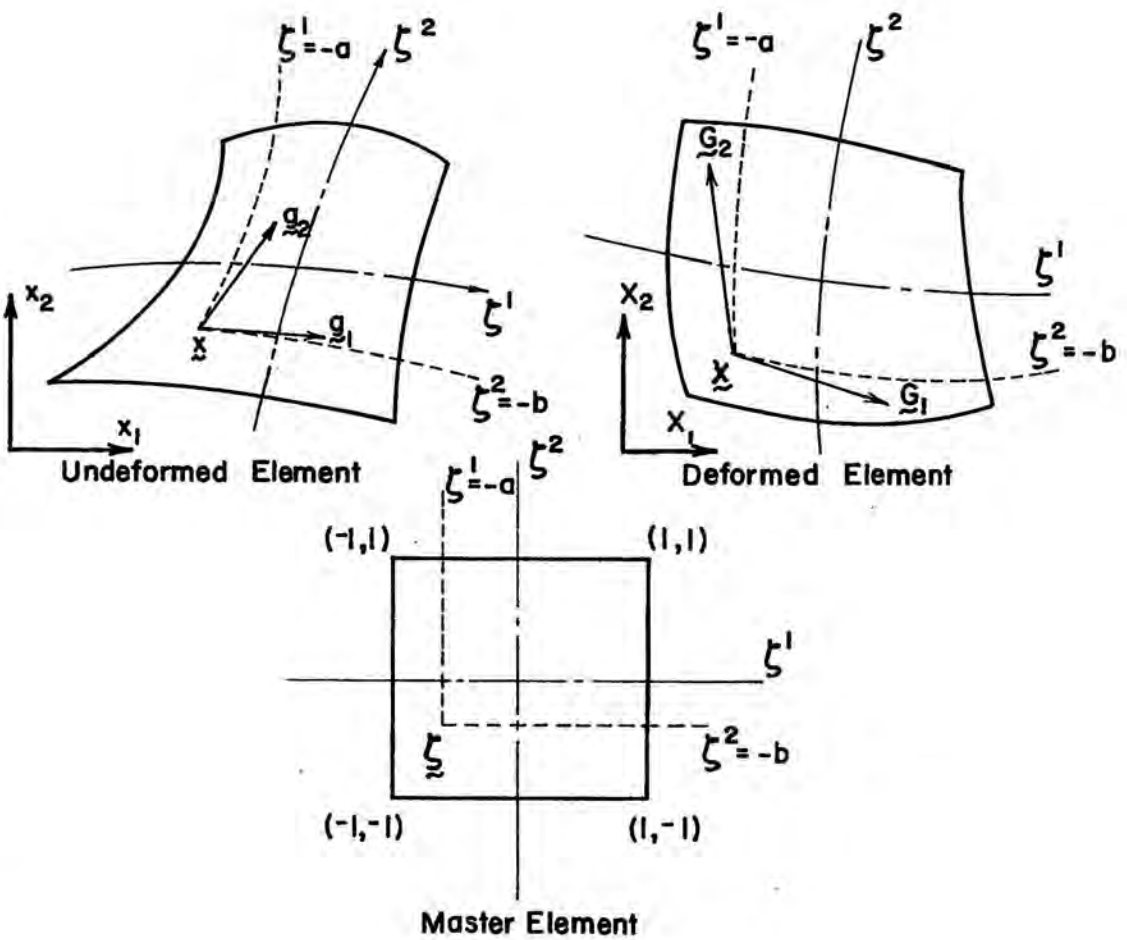

Fig. (2.2) Master Element, Undeformed Element and Deformed Element

configurations. On these elements we show the images of the lines $\zeta^1 = -a$ and $\zeta^2 = -b$ of the master element. The figure also shows the covariant base vectors $(\underset{\sim}{g}_k, \underset{\sim}{G}_k)$ at points $(\underset{\sim}{x})$ and $(\underset{\sim}{X})$, which are tangential to the coordinate lines (ζ^k = constant) at these points.

2.3.1 The Types of Elements Used

2.3.1.1 Elements for the Displacement Models.

The following classical [34] elements are used, the only variable being the nodal displacements (or coordinates).

1. The eight-node Serendipity element.
2. The nine-node Lagrangian element.
3. The six-node triangular element.

In each case, the shape functions contain complete polynomials of the second degree in ζ^1 and ζ^2--plus in cases 1 and 2 some additional terms of higher degree. In case 2 the shape functions are tensor products of quadratics, i.e., biquadratics. In all cases the elements are conforming (C^0).

2.3.1.2 Elements for the Mixed Models.

Here we have both the displacement and the Lagrange multiplier as variables, with the multiplier (λ or P) being a pressure-like variable which is simply called the pressure.

For the displacement, the shape functions of the previous section are used, while the pressure is "superimposed" on these elements. The pressure distribution may assume one of the following forms (Fig. (2.3)):

1. conforming (C^0), if it is descritized with the finite element corner values as variables.
2. nonconforming; for the quadrilaterial elements (eight or nine nodes) the pressure may assume linear distribution within the element, instead of the bilinear distribution assumed in the conforming case. So the number of pressure variables is (three) one less than the conforming case. The variables in our formulation were assumed to be the magnitude of the pressure at the centroid of the master element and the slopes of the linear pressure about the two centroidal axes. The elements with nonconforming pressure are called nonconforming elements.

Fig. (2.3) gives the shape functions (M^J) for both the conforming and nonconforming cases. The nonconforming elements were suggested by Professor Oden, during the course of this work.

$$\lambda = \sum_{i=1}^{4} \lambda_i M_i$$

$$M_1 = \tfrac{1}{4}(1-\zeta^1)(1-\zeta^2)$$

$$M_2 = \tfrac{1}{4}(1+\zeta^1)(1-\zeta^2)$$

$$M_3 = \tfrac{1}{4}(1-\zeta^1)(1-\zeta^2)$$

$$M_4 = \tfrac{1}{4}(1-\zeta^1)(1+\zeta^2)$$

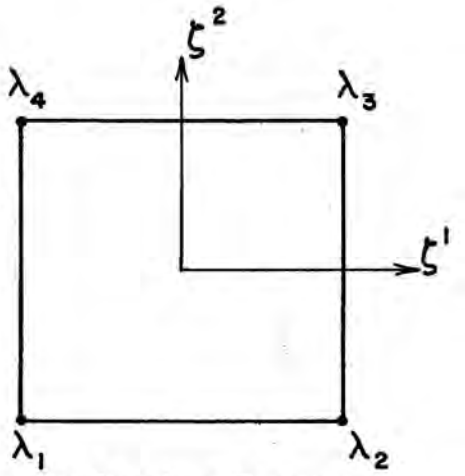

Conforming Pressure
(Bilinear)

$$\lambda = \lambda_0 M_0 + \lambda_1 M_1 + \lambda_2 M_2$$

$$M_0 = 1$$

$$M_1 = \zeta^1$$

$$M_2 = \zeta^2$$

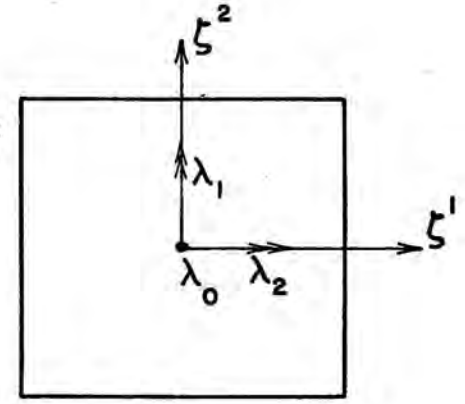

Nonconforming Pressure
(Linear)

Fig.(2.3) Pressure Interpolations

2.3.2 Numerical Integration

Gauss quadrature rules [34] are used to evaluate the various terms appearing in the virtual work statement and its linearized (rate) form. The integration is performed over the master element in the (ζ) system.

We use either of two types of integration; namely:

1. Uniform Integration Rule; in which all the terms are integrated with the same quadrature rule.
2. Reduced/Mixed Integration Rule; in which some of the terms (e.g., penalty terms) appearing in the tangent stiffness are integrated using a quadrature rule of lower order than is used for the rest of the terms.

For the quadrilateral elements we use both 9-point and 4-point integration rules, and for the triangular element we have both 7-point and 4-point integration rules. The location and weight associated with each integration point, for the various rules used, can be found in [34].

C H A P T E R I I I

FORMULATION OF THE ELEMENT MATRICES

3.1 Introduction

In this chapter we formulate the finite element matrices for both the displacement and mixed models. The calculations cover the tangent matrices $\underset{\approx}{K}_T$ and load matrices $\underset{\approx}{K}_L$, the latter being results from loads that depend on the deformations. For tangent matrices we consider the following cases:

1. the three dimensional case;
2. the plane strain case;
3. the axisymmetric case.

The load matrices are derived for:

1. pressure loading acting on an axisymmetric body;
2. pressure loading acting on a plane strain body;
3. body force loading due to the rotation of an axisymmetric body around its centroidal axis.

In the derivation of these matrices we consider separately the two terms in the virtual work (the equilibrium) equation. The first part consists of the internal virtual work δV and the second part the external

virtual work δW. The total virtual work [PVW] is given by

$$[PVW] = \delta V - \delta W \tag{3.1}$$

and its rate form is given by

$$d[PVW] = d[\delta V] - d[\delta W] \, . \tag{3.2}$$

Tangent matrices are derived from the rate of the internal virtual work and load matrices are derived from the rate of the external virtual work. The notation conventions of (2.1.1) are used here, with (ζ) being the master element $(\hat{\Omega})$ local coordinate system.

3.2 Forms of $\underset{\approx}{K}_T$

We give the tangent stiffness derivations for both the displacement and mixed models.

3.2.1 The Displacement Models

In this case the material can be compressible or nearly incompressible. In the sense of continuum

mechanics there is no distinction between "compressible" and "nearly incompressible." In both cases the energy is a function of all three invariants. Stress is completely determined by the deformation. However our interest here is for materials that are very stiff, i.e., have large ratio of bulk to shear modulii. Other engineering fields (biomedical) may have more interest in compressible materials; the formulation given below includes such materials as a special case.

The rate of the internal virtual work $d[\delta V]$ is given by

$$d[\delta V] = d[\int_{\Omega_0} \delta U \, dv_o] \tag{3.3}$$

and to determine δU and hence $d[\delta V]$ we note

1. The strain energy U is given as a function of three strain invariants.
2. The strain invariants are functions of metric tensors (2.13) (2.14) and (2.15).
3. The metric tensors at a point in the deformed or undeformed grids are functions of the coordinates of that point, relative to a fixed coordinate system.

4. The current coordinates are related to the displacements (2.4).

So

$$\delta U = \frac{\partial U}{\partial u_\alpha}\,\delta u_\alpha$$

$$= \frac{\partial U}{\partial I_k}\,\frac{\partial I_k}{\partial u_\alpha}\,\delta u_\alpha \qquad (3.4)$$

and

$$d[\delta V] = \int_{\Omega_o}\left\{\frac{\partial^2 U}{\partial u_\alpha \partial u_\beta}\,\delta u_\alpha\, du_\beta\right\} dv_o$$

$$= \int_{\Omega_o}\left\{\left[\frac{\partial^2 U}{\partial I_i \partial I_j}\,\frac{\partial I_i}{\partial u_\alpha}\,\frac{\partial I_j}{\partial u_\beta} + \frac{\partial U}{\partial I_i}\,\frac{\partial^2 I_i}{\partial u_\alpha \partial u_\beta}\right]\delta u_\alpha\, du_\beta\right\} dv_o \qquad (3.5)$$

Note that the dependence in item (1) is the only place that the development depends on the particular material being considered. The separation of this dependence, which is of a comparatively simple form, allows a completely general development of the remainder of the equations and their coding.

Now introduce the finite element interpolation for the (α) component of displacement ($\underline{u}$)

$$u_\alpha = \sum_{i=1}^{NODE} N^i \, u_\alpha^i \qquad (3.6)$$

where

u_α^i is the (α) component of displacement at node i; and i runs from one to the total number of nodes (NODE).

Equation (3.5) can then be written inthe form

$$d[\delta V] = [K_T]_{rs}^{\alpha\beta} \, \delta u_\alpha^r \, du_\beta^s \qquad (3.7a)$$

where the tangent matrix $\underset{\sim}{K}_T$ is given by

$$[K]_{rs}^{\alpha\beta} = \int_{\Omega_0} \left[\frac{\partial^2 U}{\partial I_i \, \partial I_j} \frac{\partial I_i}{\partial u_\alpha^r} \frac{\partial I_j}{\partial u_\beta^s} + \frac{\partial U}{\partial I_i} \frac{\partial^2 I_i}{\partial u_\alpha^r \, \partial u_\beta^s} \right] dv_0 \cdot \qquad (3.7b)$$

Note that for nearly incompressible materials, energy forms include bulk terms such as

$$\frac{1}{\varepsilon}(I_3 - 1)^2, \quad \frac{1}{\varepsilon}(\sqrt{I_3} - 1)^2 \text{ and } \frac{1}{\varepsilon}(\mathrm{Ln}(I_3))^2 \, .$$

These terms are more often called penalty terms. They need to be integrated in a different manner than the rest

of the energy form; otherwise "locking" may occur. In our formulation we use reduced integration similar to what is given in [34] to overcome the "locking" difficulty. Other methods for dealing with this difficulty can also be found in [12] and [16]. Penalty terms with reduced integration may be thought of in two different ways:

1. The penalty is a device for enforcing the constraint of incompressibility, and we should (but of course we can not) let

$$\frac{1}{\varepsilon} \to \infty.$$

2. The penalty terms are "bulk" energy terms--$1/\varepsilon$ has a fixed value that could be determined experimentally, and we use reduced integration to avoid numerical difficulties imposed by finite word length on our computers.

Before we start the mixed-model formulation we comment on the choice of an energy form appropriate for compressible materials. In this context the ideas given by Majerus [15] and Cheng [5] were useful. They suggested that a compressible energy form must result in a stress-free state at the initial conditions and be positive definite. See the appendix for some details. Implementing these ideas, Skala [28] suggested a modified (compressible) neo-Hookean constitutive law of the form

$$U = c_1(\tilde{I}_1 - 3) + c_3(\sqrt{I_3} - 1)^2 \ .$$

Also Cescotto et al. [6] suggested a modified Mooney constitutive law of the form

$$U = c_1(\tilde{I}_1 - 3) + c_2(\tilde{I}_2 - 3) + c_3(I_3 - 1)^2$$

where

$$\tilde{I}_1 = I_1 - I_3 - 2 \quad \text{and} \quad \tilde{I}_2 = I_2 - 2I_3 - 1 \ .$$

Both Skala and Cescotto related the coefficients in the energy form to the infinitesimal initial elasticity coefficients (the shear and bulk modulii).

Comments: It is to be noted that the energy forms used by Skala and Cescotto et al. do not satisfy one obvious requirement for constitutive models of compressible materials. That is, U does increase without bound as I_3 approaches zero. In other words, for a compressible material we must have $U \to \infty$ as $I_3 \to 0$. One way to make the above mentioned constitutive laws satisfy this requirement is by adding to these laws a logarithmic term of the form $-\varepsilon \, \mathrm{Ln}(\sqrt{I_3})$, with ε being a small number. If the ratio of bulk to shear modulii is large, however, I_3 is often far from +0, even without the use of the logarithmic term.

3.2.2 The Mixed Models

In this case the incompressibility condition is

imposed by means of the Lagrange multiplier. Here the energy function U (Eq. 3.4) is replaced by U^M. The function U^M is related to U as follows:

1--The Multiplier Method [14]

$$U^M = U + \lambda h \qquad (3.8a)$$

where (λh) is a multiplier function.

2--The Augmented Lagrangian Method [24, 32]

$$U^M = U + \lambda h + Rh^2 \qquad (3.8b)$$

where

λ is the Lagrange multiplier

R is a regularizing parameter

$h = 0$ is the constraint equation.

So in the Augmented Lagrangian method the constraint is to be satisfied by the use of a multiplier and a penalty functions, however (R) need not be very large. Possible choices for h are

$$(I_3 - 1),\ (\sqrt{I_3} - 1) \text{ and } -\mathrm{Ln}(\sqrt{I_3}) .$$

The meaning of λ for a given (Mooney as an example) constitutive law depends on the choice of (h) as illustrated below

$$1.\quad U_1^M = c_1(I_1 - 3) + c_2(I_2 - 3) + \lambda_1(I_3 - 1)$$

$$2.\quad U_2^M = c_1(I_1 - 3) + c_2(I_2 - e) + \lambda_2(\sqrt{I_3} - 1)$$

$$3.\quad U_3^M = c_1(I_1 - 3) + c_2(I_2 - 3) - \lambda_3(\mathrm{Ln}\,(\sqrt{I_3}))\,.$$

At the initial conditions ($I_1 = I_2 = 3$, $I_3 = 1$), the stresses calculated using any of the above forms are the same for the following two cases (refer to section 2.1.1).

(a) The compressible stress equations

$$(\tau^{ij})_k = \phi\, g^{ij} + \psi\, B^{ij} + \left(2\sqrt{I_3}\,\frac{\partial U_k^M}{\partial I_3}\right) G^{ij} \qquad (3.9a)$$

(b) The incompressible stress equations

$$\tau^{ij} = \hat{\phi}\, g^{ij} + \hat{\psi}\, B^{ij} + PG^{ij} \qquad (3.9b)$$

where P is the hydrostatic pressure.

At the initial conditions we have

$$\hat{\phi} = \phi$$

$$\hat{\psi} = \psi$$

Thus comparing (3.9a) and (3.9b) we get

$$\lambda_1 = \frac{P}{2}\ , \quad \lambda_2 = P \quad \text{and} \quad \lambda_3 = -P\ .$$

In most of the mixed-model formulations reported [2, 21, 27], the constraint equation (λh) took the following form

$$\lambda h(I_3) = \frac{P}{2}(I_3 - 1)$$

which directly means that the multiplier is half the hydrostatic pressure, when the constraint is expressed as $I_3 - 1 = 0$.

In (3.8a) or (3.8b), we have U^M is a function of the pair (u_α, λ). The first variation of U^M is given by

$$\delta U^M = \frac{\partial U^M}{\partial u_\alpha}\,\delta u_\alpha + \frac{\partial U^M}{\partial \lambda}\,\delta\lambda\ . \tag{3.10}$$

And the rate of internal virtual work is

$$d[\delta V^M] = \int_{\Omega_o} \left[\frac{\partial^2 U^M}{\partial u_\alpha \partial u_\beta} \delta u_\alpha \, du_\beta + \frac{\partial^2 U^M}{\partial u_\alpha \partial \lambda} \delta u_\alpha \, d\lambda + \frac{\partial^2 U^M}{\partial \lambda \partial u_\beta} \delta\lambda \, du_\beta + \frac{\partial^2 U^M}{\partial \lambda \partial \lambda} \delta\lambda \, d\lambda \right] dv_o \qquad (3.11)$$

The previous form of $d[\delta V]$ may be written as follows

$$d[\delta V^M] = [\delta u_\alpha \quad \delta\lambda] \begin{bmatrix} [\underset{\approx}{K}]^{\alpha\beta} & [\underset{\approx}{K}]^{\alpha\lambda} \\ [\underset{\approx}{K}]^{\lambda\beta} & [\underset{\approx}{K}]^{\lambda\lambda} \end{bmatrix} \begin{bmatrix} du_\beta \\ d\lambda \end{bmatrix} . \qquad (3.12)$$

For $\alpha = \beta$

$$[\underset{\approx}{K}]^{\alpha\lambda} = [\underset{\approx}{K}^T]^{\lambda\beta} \qquad (3.13)$$

where (T) means transpose; and for the particular choices of U^M given in items (1), (2) and (3)

$$[\underset{\approx}{K}]^{\lambda\lambda} = \underset{\approx}{0} \; . \qquad (3.14)$$

Now introduce the finite element interpolations for both the displacement and pressure.

For the displacement

$$u_\alpha = \sum_{i=1}^{NODE} N^i u_\alpha^i \; . \qquad (3.15)$$

For the pressure

$$\lambda = \sum_{j=1}^{NP} M^j \lambda^j \qquad (3.16)$$

where

N^i are the shape functions for interpolating the displacement (u_α)

M^j are the shape functions for interpolating the pressure

NODE is the total number of nodes on the element used

NP is the total number of pressure variables in the element used.

Substituting (3.13) through (3.16) in (3.12) we get

$$d[\delta V^M] = \begin{bmatrix} \delta u_\alpha^i & \delta \lambda^k \end{bmatrix} \begin{bmatrix} K_{ij}^{\alpha\beta} & \text{Sym.} \\ K_{kj}^{\lambda\beta} & 0 \end{bmatrix} \begin{bmatrix} du_\beta^j \\ d\lambda^k \end{bmatrix} \qquad (3.17)$$

where

i,j runs from one to NODE

k runs from one to NP

and the matrices $K_{ij}^{\alpha\beta}$ and $K_{kj}^{\lambda\beta}$ are given by

$$K_{ij}^{\alpha\beta} = \int_{\Omega_0} \frac{\partial^2 U^M}{\partial u_\alpha^i \, \partial u_\beta^j} \, dv_0$$

$$= \int_{\Omega_0} \left[\frac{\partial^2 U^M}{\partial I_r \, \partial I_s} \frac{\partial I_r}{\partial u_\alpha^i} \frac{\partial I_s}{\partial u_\beta^j} + \frac{\partial U^M}{\partial I_r} \frac{\partial^2 I_r}{\partial u_\alpha^i \, \partial u_\beta^j} \right] dv_0 \qquad (3.18)$$

$$K_{kj}^{\lambda\beta} = \int_{\Omega_0} \frac{\partial^2 U^M}{\partial \lambda^k \, \partial u_\beta^j} \, dv_0 \qquad (3.19a)$$

Since in (3.8a) or (3.8b) the only term which depends on λ is (λh) then

$$K_{kj}^{\lambda\beta} = \int_{\Omega_0} \frac{\partial^2 (\lambda h)}{\partial \lambda^k \, \partial u_\beta^j} \, dv_0 \, . \qquad (3.19b)$$

Using (3.16) we get

$$K_{kj}^{\lambda\beta} = \int_{\Omega_0} \left[M^k \frac{\partial (h(I_3))}{\partial u_\beta^j} \right] dv_0 \qquad (3.19c)$$

$$= \int_{\Omega_0} \left[M^k \frac{\partial h(I_3)}{\partial I_r} \frac{\partial I_r}{\partial u_\beta^j} \right] dv_0 \, . \qquad (3.19d)$$

It is easy to see that the size of the submatrix $\underset{\approx}{K}^{\alpha\beta}$ of the mixed model (3.18) is the same as the size of the whole matrix obtained in the displacement model (3.7b).

It is to be noted that, firstly because the constraint equation (2.21) is nonlinear and secondly

because we use an iterative scheme based on linearization of the equilibrium and constraint equations, the constraint is only satisfied at a solution point. That is to say the results obtained after, for example, the first iteraction are compressible. From this viewpoint a compressible energy form may be augmented with a multiplier or augmented Lagrangian functions and used for incompressible (mixed) formulation.

To make this idea clear, we note that (E_0), the true initial tangent modulus (Young's modulus) for incompressible materials, is not affected by the third system invariant and is given by

$$E_0 = 6(U,_1 + U,_2)_0$$

where the subscript (0) means initial ($I_1 = I_2 = 3$, $I_3 = 1$) and

$$U,_1 = \frac{\partial U}{\partial I_1} \quad , \quad U,_2 = \frac{\partial U}{\partial I_2} \ .$$

But the computed initial tangent is affected by the third strain invariant (see the appendix for some details). So we could, if desired, augment the incompressible energy

form with functions of the third strain invariant and adjust the computed initial tangent to be equal to, or of the same order of, the true initial tangent.

3.3 Details of the Calculations

It is apparent that to calculate the tangent stiffness matrices we need to calculate the following quantities:

1. The first and second derivatives of the strain energy function with respect to the three strain invariants. This is not difficult since the strain energy is assumed to be given as an explicit function of the strain invariants.
2. The first and second derivatives of the strain invariants with respect to the nodal displacements. This is more tedious, but these calculations do not change from one material to another. so they are calculated once and for all. The details are given in the following three sections, for the three-dimensional, the plane strain and the axisymmetric cases.

3.3.1 The Three-Dimensional Case

The metric tensors are given by

$$g_{k\ell} = \frac{\partial x_\alpha}{\partial \zeta^k} \frac{\partial x_\alpha}{\partial \zeta^\ell} \tag{3.20}$$

$$G_{k\ell} = \frac{\partial X_\alpha}{\partial \zeta^k} \frac{\partial X_\alpha}{\partial \zeta^\ell} \tag{3.21}$$

and the strain invariants are given by

$$I_1 = g^{k\ell} G_{k\ell} \tag{3.22}$$

$$I_2 = g_{k\ell} G^{k\ell} I_3 \tag{3.23}$$

$$I_3 = \frac{G}{g} \quad . \tag{3.24}$$

For the first and second derivatives of the strain invariants with respect to the finite element nodal displacements we have

1. For the first strain invariant

$$\frac{\partial I_1}{\partial u_\alpha^i} = g^{k\ell} \left(\frac{\partial N^i}{\partial \zeta^k} \frac{\partial X_\alpha}{\partial \zeta^\ell} + \frac{\partial X_\alpha}{\partial \zeta^k} \frac{\partial N^i}{\partial \zeta^\ell} \right) \tag{3.25}$$

$$\frac{\partial^2 I_1}{\partial u_\alpha^i \, \partial u_\beta^j} = 2g^{k\ell}\left(\frac{\partial N^i}{\partial \zeta^k}\,\frac{\partial N^j}{\partial \zeta^\ell}\right)\ \delta_{\alpha\beta} \tag{3.26}$$

where

$$\delta_{\alpha\beta} = 1 \text{ if } \alpha = \beta;$$
$$= 0 \text{ if } \alpha \neq \beta.$$

2. For the third strain invariant

$$\frac{\partial I_3}{\partial u_\alpha^i} = \frac{1}{g}\,\frac{\partial G}{\partial u_\alpha^i}$$

$$= \frac{1}{g}\,\frac{\partial}{\partial u_\alpha^i}\left(\frac{1}{6}\,\epsilon_{pqr}\,\epsilon_{k\ell m}\,G_{pk}\,G_{q\ell}\,G_{rm}\right)$$

$$= \frac{1}{g}\,\frac{\partial}{\partial G_{st}}\left(\frac{1}{6}\,\epsilon_{pqr}\,\epsilon_{k\ell m}\,G_{pk}\,G_{q\ell}\,G_{rm}\right)\frac{\partial G_{st}}{\partial u_\alpha^i}$$

$$= \frac{1}{g}\left(\frac{1}{2}\,\epsilon_{sqr}\,\epsilon_{t\ell m}\,G_{q\ell}\,G_{rm}\right)$$

$$\times\left(\frac{\partial N^i}{\partial \zeta^s}\,\frac{\partial X_\alpha}{\partial \zeta^t} + \frac{\partial X_\alpha}{\partial \zeta^s}\,\frac{\partial N^i}{\partial \zeta^t}\right) \tag{3.27}$$

$$\frac{\partial^2 I_3}{\partial u_\alpha^i \, \partial u_\beta^j} = \frac{1}{g}\Bigg[\Bigg(\epsilon_{ser}\,\epsilon_{tnm}\,G_{rm}$$

$$\times\left(\frac{\partial N^j}{\partial \zeta^e}\,\frac{\partial X_\beta}{\partial \zeta^n} + \frac{\partial X_\beta}{\partial \zeta^e}\,\frac{\partial N^j}{\partial \zeta^n}\right)\left(\frac{\partial N^i}{\partial \zeta^s}\,\frac{\partial X_\alpha}{\partial \zeta^t} + \frac{\partial X_\alpha}{\partial \zeta^s}\,\frac{\partial N^i}{\partial \zeta^t}\right)$$

$$+\left(\frac{1}{2}\,\epsilon_{sqr}\,\epsilon_{t\ell m}\,G_{q\ell}\,G_{rm}\right)\left(\frac{\partial N^i}{\partial \zeta^s}\,\frac{\partial N^j}{\partial \zeta^t} + \frac{\partial N^j}{\partial \zeta^s}\,\frac{\partial N^i}{\partial \zeta^t}\right)\Bigg] \tag{3.28}$$

where

$\epsilon_{ijk} = 1$ if i, j, k is an even permutation of the numbers 1, 2, 3;

$= -1$ if i, j, k is an odd permutation of the numbers 1, 2, 3;

$= 0$ if two of the indices are equal.

3. For the second strain invariant

$$\frac{\partial I_2}{\partial u_\alpha^i} = \frac{\partial}{\partial u_\alpha^i}\left(g_{k\ell}\ G^{k\ell}\ \frac{G}{g}\right)$$

$$= \frac{g_{k\ell}}{g}\ \frac{\partial}{\partial u_\alpha^i}\ (\text{adj}\ G_{k\ell})$$

$$= \frac{g_{k\ell}}{g}\ \frac{\partial}{\partial u_\alpha^i}\left(\frac{1}{2}\ \epsilon_{kpq}\ \epsilon_{\ell rs}\ G_{pr}\ G_{qs}\right)$$

$$= \frac{g_{k\ell}}{g}\ (\epsilon_{ktq}\ \epsilon_{\ell ms}\ G_{qs})\left(\frac{\partial N^i}{\partial \zeta^t}\ \frac{\partial X_\alpha}{\partial \zeta^m}\right.$$

$$\left. + \frac{\partial X_\alpha}{\partial \zeta^t}\ \frac{\partial N^i}{\partial \zeta^m}\right) \qquad (3.29)$$

$$\frac{\partial^2 I_2}{\partial u_\alpha^i\ \partial u_\beta^j} = \frac{g_{k\ell}}{g}\left[\epsilon_{kte}\ \epsilon_{\ell mn}\left(\frac{\partial N^j}{\partial \zeta^e}\ \frac{\partial X_\beta}{\partial \zeta^n} + \frac{\partial X_\beta}{\partial \zeta^e}\ \frac{\partial N^j}{\partial \zeta^n}\right)\left(\frac{\partial N^i}{\partial \zeta^t}\ \frac{\partial X_\alpha}{\partial \zeta^m}\right.\right.$$

$$\left.\left. + \frac{\partial X_\alpha}{\partial \zeta^t}\ \frac{\partial N^i}{\partial \zeta^m}\right) + \epsilon_{ktq}\ \epsilon_{\ell ms}\ G_{qs}\left(2\ \frac{\partial N^i}{\partial \zeta^t}\ \frac{\partial N^j}{\partial \zeta^m}\right)\delta_{\alpha\beta}\right]. \qquad (3.30)$$

3.3.2 The Plane Strain Case

Here we choose $\zeta^3 = x_3 = X_3$; so that

$$g_{33} = \frac{\partial x_k}{\partial x_3} \cdot \frac{\partial x_k}{\partial x_3} = 1.$$

$$G_{33} = \frac{\partial X_k}{\partial x_3} \cdot \frac{\partial X_k}{\partial x_3} = 1.$$

And

$$g_{31} = g_{32} = g_{23} = g_{13} = 0. \tag{3.31}$$

$$G_{31} = G_{32} = G_{23} = G_{13} = 0. \tag{3.32}$$

$$g^{12} = -g_{12},\ g^{21} = -g_{21} \tag{3.33}$$

$$G^{12} = -G_{12},\ G^{21} = -G_{21}. \tag{3.34}$$

The other metric tensor components are given by

(a) For the undeformed body

$$g_{11} = \left(\frac{\partial x_1}{\partial \zeta^1}\right)^2 + \left(\frac{\partial x_2}{\partial \zeta^1}\right)^2 \tag{3.35}$$

$$g_{22} = \left(\frac{\partial x_1}{\partial \zeta^2}\right)^2 + \left(\frac{\partial x_2}{\partial \zeta^2}\right)^2 \tag{3.36}$$

$$g_{12} = \frac{\partial x_1}{\partial \zeta^1}\frac{\partial x_1}{\partial \zeta^2} + \frac{\partial x_2}{\partial \zeta^1}\frac{\partial x_2}{\partial \zeta^2} \quad . \tag{3.37}$$

And the determinant g is given by

$$g = g_{11}\, g_{22} - g_{12}^2 \tag{3.38}$$

(b) For the deformed body

$$G_{11} = \left(\frac{\partial X_1}{\partial \zeta^1}\right)^2 + \left(\frac{\partial X_2}{\partial \zeta^1}\right)^2 \tag{3.39}$$

$$G_{22} = \left(\frac{\partial X_1}{\partial \zeta^2}\right)^2 + \left(\frac{\partial X_2}{\partial \zeta^2}\right)^2 \tag{3.40}$$

$$G_{12} = \frac{\partial X_1}{\partial \zeta^1}\frac{\partial X_1}{\partial \zeta^2} + \frac{\partial X_2}{\partial \zeta^1}\frac{\partial X_2}{\partial \zeta^2} \quad . \tag{3.41}$$

And the determinant G is given by

$$G = G_{11}\, G_{22} - G_{12}^2 \tag{3.42}$$

the strain invariants become

$$I_1 = \frac{1}{g}\,(g_{11}\, G_{22} + g_{22}\, G_{11} - 2\, g_{12}\, G_{12} + g) \tag{3.43}$$

$$I_2 = \frac{1}{g} \left(g_{11} G_{22} + g_{22} G_{11} - 2 g_{12} G_{12} + G\right) \tag{3.44}$$

$$I_3 = \frac{G}{g} = \frac{1}{g} \left(G_{11} G_{22} - G_{12}^2\right) \tag{3.45}$$

and their derivatives with respect to the nodal displacements are given by

1. For the first strain invariant

$$\frac{\partial I_1}{\partial u_\alpha^i} = \frac{2}{g} \left[\left(g_{22} \frac{\partial X_\alpha}{\partial \zeta^1} - g_{12} \frac{\partial X_\alpha}{\partial \zeta^2}\right) \frac{\partial N^i}{\partial \zeta^1} + \left(g_{11} \frac{\partial X_\alpha}{\partial \zeta^2} - g_{12} \frac{\partial X_\alpha}{\partial \zeta^1}\right) \frac{\partial N^i}{\partial \zeta^2}\right] \tag{3.46}$$

$$\frac{\partial^2 I_1}{\partial u_\alpha^i \, \partial u_\beta^j} = \frac{2\delta_{\alpha\beta}}{g} \left[g_{22} \frac{\partial N^i}{\partial \zeta^1} \frac{\partial N^j}{\partial \zeta^1} - g_{12} \left(\frac{\partial N^i}{\partial \zeta^2} \frac{\partial N^j}{\partial \zeta^1} + \frac{\partial N^j}{\partial \zeta^2} \frac{\partial N^i}{\partial \zeta^1}\right) + g_{11} \frac{\partial N^i}{\partial \zeta^2} \frac{\partial N^j}{\partial \zeta^2}\right] \tag{3.47}$$

2. For the third strain invariant

$$\frac{\partial I_3}{\partial u_\alpha^i} = \frac{2}{g} \left[\left(G_{22} \frac{\partial X_\alpha}{\partial \zeta^1} - G_{12} \frac{\partial X_\alpha}{\partial \zeta^2}\right) \frac{\partial N^i}{\partial \zeta^1} + \left(G_{11} \frac{\partial X_\alpha}{\partial \zeta^2} - G_{12} \frac{\partial X_\alpha}{\partial \zeta^1}\right) \frac{\partial N^i}{\partial \zeta^2}\right] \tag{3.48}$$

The second derivatives are

(a) For $\alpha = \beta$

$$\frac{\partial^2 I_3}{\partial u_\alpha^i \, \partial u_\beta^j} = \frac{2}{g} \left[\left(G_{22} - \left(\frac{\partial X_\alpha}{\partial \zeta^2} \right)^2 \right) \frac{\partial N^i}{\partial \zeta^1} \frac{\partial N^j}{\partial \zeta^1} + \left(\frac{\partial X_\alpha}{\partial \zeta^1} \frac{\partial X_\alpha}{\partial \zeta^2} - G_{12} \right) \frac{\partial N^i}{\partial \zeta^2} \frac{\partial N^j}{\partial \zeta^1} + \left(\frac{\partial X_\alpha}{\partial \zeta^1} \frac{\partial X_\alpha}{\partial \zeta^2} - G_{12} \right) \frac{\partial N^i}{\partial \zeta^1} \frac{\partial N^j}{\partial \zeta^2} + \left(G_{11} - \left(\frac{\partial X_\alpha}{\partial \zeta^1} \right)^2 \right) \frac{\partial N^i}{\partial \zeta^2} \frac{\partial N^j}{\partial \zeta^2} \right] \quad (3.49)$$

No sum on α

(b) For $\alpha \neq \beta$

Let

$$u_\alpha = v, \; u_\beta = u$$

$$X_\alpha = Y, \; X_\beta = X \; .$$

Then

$$\frac{\partial^2 I_3}{\partial v^i \, \partial u^j} = \frac{2}{g}\left[-\left(\frac{\partial X}{\partial \zeta^2}\frac{\partial Y}{\partial \zeta^2}\right)\frac{\partial N^i}{\partial \zeta^1}\frac{\partial N^j}{\partial \zeta^1} - \left(\frac{\partial Y}{\partial \zeta^1}\frac{\partial X}{\partial \zeta^1}\right)\frac{\partial N^i}{\partial \zeta^2}\frac{\partial N^j}{\partial \zeta^2}\right.$$
$$+\left(2\frac{\partial X}{\partial \zeta^2}\frac{\partial Y}{\partial \zeta^1} - \frac{\partial X}{\partial \zeta^1}\frac{\partial Y}{\partial \zeta^2}\right)\frac{\partial N^i}{\partial \zeta^1}\frac{\partial N^j}{\partial \zeta^2}$$
$$\left.+\left(2\frac{\partial Y}{\partial \zeta^2}\frac{\partial X}{\partial \zeta^1} - \frac{\partial X}{\partial \zeta^2}\frac{\partial Y}{\partial \zeta^1}\right)\frac{\partial N^i}{\partial \zeta^2}\frac{\partial N^j}{\partial \zeta^1}\right] \qquad (3.50)$$

3. For the second strain invariant

Equations (3.48), (3.44) and (3.45) imply that

$$I_2 = (I_1 - 1) + I_3. \qquad (3.51)$$

Thus the derivatives of the second strain invariant can be inferred from the derivatives of the first and third strain invariants.

3.3.3 The Axisymmetric Case

For axisymmetric problems it is easier to use a cylindrical polar coordinate system, rather than the cartesian coordinate system. Let (R,Z,θ) be the current position of a point that originally was at (r,z,θ) in the undeformed body. The underformed and deformed cartesian components are given by

$$x_1 = r \cos \theta,\ x_2 = z,\ x_3 = r \sin \theta$$

and

$$X_1 = R \cos \theta,\ X_2 = Z,\ X_3 = R \sin \theta.$$

Choose (ζ^3) the finite element coordinate line such that $\zeta^3 = \theta$. The three-three components (g_{33}, G_{33}) of the metric tensors (which had the value unity for the plane strain case) are given by

$$g_{33} = \frac{\partial x_\alpha}{\partial \theta} \frac{\partial x_\alpha}{\partial \theta} = r^2 \qquad (3.52)$$

$$G_{33} = \frac{\partial X_\alpha}{\partial \theta} \frac{\partial X_\alpha}{\partial \theta} = R^2 \ . \qquad (3.53)$$

The other components of the metric tensors ($\underset{\approx}{g}$ and $\underset{\approx}{G}$) are the same as the plane strain case; with r/R replacing x/X and z/Z replacing x/X.

The strain invariants become

$$I_1 = \frac{1}{g} (g_{11} G_{22} + g_{22} G_{11} - 2 g_{12} G_{12}) + \frac{R^2}{r^2} \qquad (3.54)$$

$$I_2 = \frac{1}{g}\left(g_{11}\, G_{22} + g_{22}\, G_{11} - 2\, g_{12}\, G_{12}\right) + \frac{G}{g} \qquad (3.55)$$

$$I_3 = \frac{R^2}{r^2}\,\frac{G}{g} = \frac{R^2}{g r^2}\left(G_{11}\, G_{22} - G_{12}^2\right) . \qquad (3.56)$$

It is obvious that the strain invariants can be written in the form

$$I_1 = \left(I_1^0 - 1\right) + \frac{R^2}{r^2} \qquad (3.57)$$

$$I_2 = \left(I_1^0 - 1\right)\frac{R^2}{r^2} + I_3^0 \qquad (3.58)$$

$$I_3 = I_3^0\,\frac{R^2}{r^2} . \qquad (3.59)$$

where the strain invariants with the superscript (0) are the strain invariants of the plane strain case. So it is easy to derive the strain invariant derivatives from the plane strain case. We only need to know that

$$\frac{\partial(R^2)}{\partial u_\alpha^i} = 2R\, N^i\, \delta_{1\alpha} \qquad (3.60)$$

$$\frac{\partial^2(R^2)}{\partial u_\alpha^i\, \partial u_\beta^j} = 2\, N^i\, N^j\, \delta_{1\alpha}\, \delta_{1\beta} . \qquad (3.61)$$

where $\delta_{1\alpha}$ and $\delta_{1\beta}$ are the Kroneker deltas.

3.4 Forms of $\underset{\sim}{K}_L$

The treatment of load stiffness given here is an implementation of the ideas given by Hibbitt [10].

3.4.1 Pressure Loading

The external virtual work (δW^p) due to pressure acting on a body is given by

$$\delta W^p = \int_{\partial\Omega_2} \underset{\sim}{p}\cdot\delta\underset{\sim}{u}\, dS \qquad (3.62)$$

where

$\partial\Omega_2$ is the part of the boundary on which the pressure (p) acts.

dS is the current incremental area of ($\partial\Omega_2$).

$\delta\underset{\sim}{u}$ is a virtual displacement.

We will assume the pressure to be positive when it acts opposite to the normal ($\underset{\sim}{n}$) of the surface ($\partial\Omega_2$) on which it acts; so that equation (3.62) is rewritten as

$$\delta W^p = -\int_{\partial\Omega_2} p\ \underset{\sim}{n}\cdot\delta\underset{\sim}{u}\, dS\ . \qquad (3.63)$$

And its rate form is given by

$$d[\delta W^p] = d \int_{\partial \Omega_2} p \, \underset{\sim}{n} \cdot \delta \underset{\sim}{u} \, dS \, . \tag{3.64}$$

Since the boundary ($\partial \Omega_2$) changes with deformation, the integration in (3.64) will be transformed to the finite element (ζ) system in which its rate form will be derived. This is achieved by writing the term ($\underset{\sim}{n} \, dS$) relative to this new system.

3.4.1.1 The Axisymmetric Case. Let ζ^2, ζ^3 be defined on the surface ($\partial \Omega_2$) on which the pressure acts, and consider a point (A), Fig. (3.1), on this surface with current position vector ($\underset{\sim}{R}$). The element of area at (A) is given by

$$\underset{\sim}{n} \, dS = d\underset{\sim}{R}_2 \times d\underset{\sim}{R}_3$$

$$= \frac{\partial \underset{\sim}{R}}{\partial \zeta^2} \times \frac{\partial \underset{\sim}{R}}{\partial \zeta^3} \, d\zeta^2 \, d\zeta^3 . \tag{3.65a}$$

Introduce a cylindrical polar coordinate system (R, Z, θ) and let $\theta = \zeta^3$, then (3.65) becomes

$$\underset{\sim}{n} \, dS = \frac{\partial \underset{\sim}{R}}{\partial \zeta^2} \times \frac{\partial \underset{\sim}{R}}{\partial \theta} \, d\zeta^2 \, d\theta \, . \tag{3.65b}$$

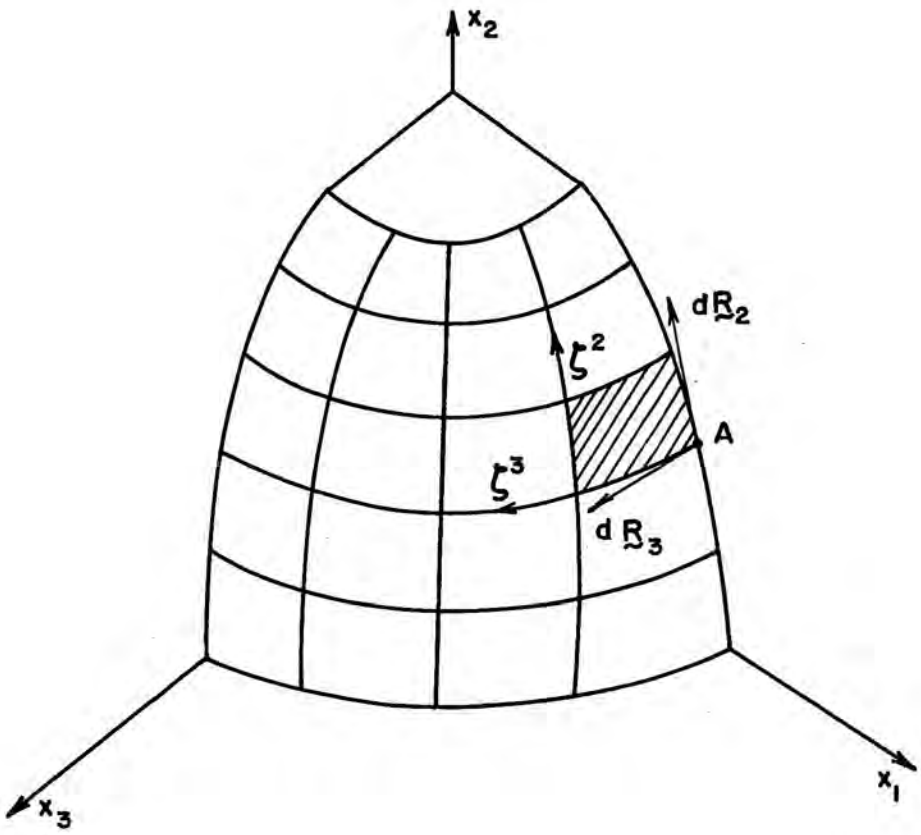

Fig. (3.1) Area Increment in the Finite Element (ζ^2, ζ^3) Coordinates

The cartesian component form of $\underset{\sim}{R}$ is

$$\underset{\sim}{R} = X_1 \underset{\sim}{i}_1 + X_2 \underset{\sim}{i}_2 + X_3 \underset{\sim}{i}_3$$

and in terms of the cylindrical coordinate system

$$\underset{\sim}{R} = R \cos \theta \, \underset{\sim}{i}_1 + Z \, \underset{\sim}{i}_2 + R \sin \theta \, \underset{\sim}{i}_3 \; ;$$

now (3.65b) becomes

$$\underset{\sim}{n} \, dS = \left(R \frac{\partial Z}{\partial \zeta^2} \cos \theta \, \underset{\sim}{i}_1 - R \frac{\partial R}{\partial \zeta^2} \, \underset{\sim}{i}_2 + R \frac{\partial Z}{\partial \zeta^2} \sin \theta \, \underset{\sim}{i}_3 \right) d\zeta^2 \, d\theta \; . \qquad (3.65c)$$

A component form of a virtual displacement ($\delta \underset{\sim}{u}$), consistent with the axisymmetric deformation, is written as

$$\delta \underset{\sim}{u} = \delta u_r \cos \theta \, \underset{\sim}{i}_1 + \delta u_z \, \underset{\sim}{i}_2 + \delta u_r \sin \theta \, \underset{\sim}{i}_3 \qquad (3.66)$$

and thus the virtual work is given by

$$\delta W^p = -\int_{\partial \hat{\Omega}} p \left[R \, \delta u_r \frac{\partial Z}{\partial \zeta^2} - R \, \delta u_z \frac{\partial R}{\partial \zeta^2} \right] d\zeta^2 \qquad (3.67)$$

where integration with respect to θ over one radian in (3.67) is understood.

The rate form of the virtual work is given by

$$d[\delta W^p] = -\int_{\partial\hat{\Omega}} p \left(du_r \, \delta u_r \frac{\partial Z}{\partial \zeta^2} + R \, \delta u_r \frac{\partial du_z}{\partial \zeta^2} - du_r \, \delta u_z \frac{\partial R}{\partial \zeta^2} - R \, \delta u_z \frac{\partial du_r}{\partial \zeta^2} \right) d\zeta^2 \, . \quad (3.68a)$$

It was Hibbitt [10] who showed that the load matrix due to pressure loading could be symmetric. Assuming that the pressure is uniform and integrating the third term in (3.68a) by parts, we get

$$d[\delta W^p] = -p\int_{\partial\hat{\Omega}} \left(du_r \, \delta u_r \frac{\partial Z}{\partial \zeta^2} + R \, \delta u_r \frac{\partial du_z}{\partial \zeta^2} + R \, du_r \frac{\partial \delta u_z}{\partial \zeta^2} \right) d\zeta^2 + BT \quad (3.68b)$$

where the boundary term, BT, is given by

$$BT = [p \, R \, \delta u_z \, du_r]$$

evaluated over the boundary of the surface on which the pressure acts. If the boundary integral vanishes, the

resulting load matrix will be symmetric. To show this let us introduce the finite element interpolations for the (r) and (z) components of the displacement

$$u_r = \sum_{i=1}^{NODE} N^i \, u_r^i$$

$$u_z = \sum_{i=1}^{NODE} N^i \, u_z^i \, .$$

The rate of the virtual work is now given by

$$d[\delta W^p] = -[\delta u_r^i \;\; \delta u_z^i] \left\{ \sum_{e \in \partial\Omega_2} \left[\underset{\approx}{K}_L^e \right] \right\} \begin{bmatrix} du_r^j \\ du_z^j \end{bmatrix} \qquad (3.69)$$

where

$\sum_{e \in \partial\Omega_2}$ means the sum over all the elements that have sides on $(\partial\Omega_2)$, on which the pressure acts,

and the load matrix $(\underset{\approx}{K}_L^e)$ is given by

$$\left[K_L^e\right]_{ij} = \int_{\partial\hat{\Omega}} \begin{bmatrix} p \dfrac{\partial Z}{\partial \zeta^2} N^i N^j & P R \dfrac{\partial N^j}{\partial \zeta^2} N^i \\ P R N^j \dfrac{\partial N^i}{\partial \zeta^2} & 0 \end{bmatrix} d\zeta^2 \qquad (3.70)$$

which is symmetric.

Note that the boundary term vanishes at an edge if the (r) or (z) component of displacement is specified for that edge. Figs. (4.2) through (4.5) satisfy this condition.

3.4.1.2 The Plane Strain Case. Here we follow the same steps for the axisymmetric case, but a cartesian coordinate system is used.

For this case $x_3 = X_3 = \zeta^3$. The external virtual work per unit length in the x_3 direction is given by

$$\delta W^p = -\int_{\partial\hat{\Omega}_2} p\left(\frac{\partial X_2}{\partial \zeta^2}\ \delta u_1 - \frac{\partial X_1}{\partial \zeta^2}\ \delta u_2\right) d\zeta^2 \qquad (3.71)$$

and its rate form (uniform pressure) is given by

$$d[\delta W^p] = -p\int_{\partial\hat{\Omega}_2}\left(\frac{\partial du_2}{\partial \zeta^2}\ \delta u_1 - \frac{\partial du_1}{\partial \zeta^2}\ \delta u_2\right)\ d\zeta^2 \ . \qquad (3.72a)$$

Again integrating the second term by parts, we get

$$d[\delta W^p] = -p\int_{\partial\hat{\Omega}_2}\left(\frac{\partial du_2}{\partial \zeta^2}\ \delta u_1 + du_1\ \frac{\partial \delta u_2}{\partial \zeta^2}\right) d\zeta^2 + BT \qquad (3.72b)$$

where the boundary term, BT, is given by

$$BT = [p\ du_1\ \delta u_2]$$

evaluated over the boundary of the surface on which the pressure acts. If the boundary term vanishes, and introducing the finite element interpolations for u_1 and u_2, the rate of the virtual work becomes

$$d[\delta W^p] = -[\delta u_1^i \quad \delta u_2^i] \left\{ \sum_{e \in \partial\Omega_2} \left[\underset{\approx}{K}_L^e \right] \right\} \begin{bmatrix} du_1^j \\ \\ du_2^j \end{bmatrix} \qquad (3.73)$$

where

$\sum_{e \in \partial\Omega_2}$ mean the sum over all the elements that have sides on $(\partial\Omega_2)$ on which the pressure acts,

and the load matrix $(\underset{\approx}{K}_L^e)$ is given by

$$\left[K_L^e\right]_{ij} = \int_{\partial\hat{\Omega}} \begin{bmatrix} 0 & pN^i \dfrac{\partial N^j}{\partial \zeta^2} \\ \\ pN^j \dfrac{\partial N^i}{\partial \zeta^2} & 0 \end{bmatrix} d\zeta^2 \qquad (3.74)$$

which is symmetric.

3.4.2 Centrifugal Loading

We treat the case of an axisymmetric body, rotating around its centroidal axis which contains the origin of the cylindrical coordinates used. The virtual work in this case is given by

$$\delta W^c = \int_{\Omega_0} (\rho_0 \ \omega^2 \ R \ \delta u_r) \ dv_0 \qquad (3.75)$$

where

ρ_0 is the mass density in the undeformed configuration.

ω is the angular speed.

u_r is the current (r) component of the point with current and original position vectors = $\underset{\sim}{R}$, $\underset{\sim}{r}$, respectively

$u_r = R - r$.

The rate of the virtual work is given by

$$d[\delta W^c] = \int_{\Omega_0} (\rho_0 \ \omega^2 \ du_r \ \delta u_r) \ dv_0 \ . \qquad (3.76)$$

Introduce the finite element interpolation

$$u_r = \sum_{i=1}^{NODE} N^i \ u_r^i .$$

Then

$$d[\delta W^c] = [\delta u_r^i] \left\{ \sum_{e \in \Omega} \left[\underset{\sim}{K}_L^e \right] \right\} [du_r^j] \qquad (3.77)$$

where

$\sum_{e \in \Omega}$ means the sum over all the elements of the body.

The load matrix $(\underset{\approx}{K}^e_L)$ is given by

$$\left[K^e_L\right]_{ij} = \int_{\hat{\Omega}} \rho_0 \, (\omega^2 \, N^i \, N^j) \, \text{Jac} \, d\zeta \qquad (3.78)$$

where

Jac is the jacobian of the transformation that maps

$\zeta \rightarrow \underset{\sim}{x}$.

C H A P T E R I V

APPLICATIONS

4.1 Pressurized Cylinder

4.1.1 Problem Description

This problem is concerned with the solution of a plane strain cylinder, of incompressible Mooney material, subjected to internal pressure, Fig. (4.1). The problem, which has an exact solution in Green and Zerna [8], was also treated using mixed finite element models by

1. Oden and Key [21]
2. Scharnhorst and Pian [27]
3. R. C. Batra [2].

The data used was

Interior radius	= 7.0"
Exterior radius	= 18.625"
Internal pressure	= 150 psi

Mooney coefficients are

$$c_1 = 80 \text{ psi}, \quad c_2 = 20 \text{ psi}.$$

A similar problem with different data was treated by Skala [29] who used a displacement finite element model.

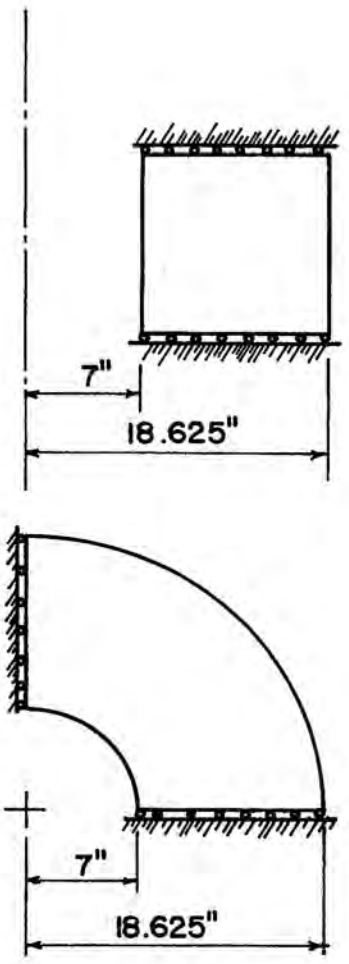

Data

Internal Pressure : 150 psi

Mooney Coefficients:

c_1 = 80 psi

c_2 = 20 psi

Fig. (4.1) Pressurized Cylinder: Dimensions and Boundary Conditions

An important feature of this problem is that the pressure acts on the deformed shape, which is not known in advance. A consistent treatment of the external virtual work due to pressure requires, beside the tangent matrix, the use of a load matrix derived from the external virtual work.

4.1.2 Plan for Discussion

In our treatment for the problem, we considered the following points:

1. We solve the problem using a grid with five axisymmetric elements and compare the results with the exact solution.
2. We compare our results with the previous results. Here we also show the importance of the load matrix. Three grids are used: a plane strain nine-element grid, an axisymmetric one-element grid and an axisymmetric five-element grid.
3. We compare the results obtained using mixed and displacement models. For this case, we use two grids: axisymmetric one-element grid and plane strain nine-element grid.

4. We compare the mixed eight-node Serendipity element and nine-node Lagrangian element, with the pressure within each element being linear (non-conforming) and bilinear (conforming). For this comparison, both the axisymmetric one-element and five-element grids are used.
5. We compare the four-point integration rule to a higher order integration rule. Both the plane strain grid and one other irregular grid are used, with the latter grid consisting of both triangular and quadrilateral elements. This is intended to show the ability to use two element types in the same grid.

In all we have four different grids. The undeformed and deformed shapes (p = 150 psi) are shown in Figs. (4.2), (4.3), (4.4), and (4.5).

4.1.3 Problem Solution

A grid with five elements, nine-point integration rule and conforming pressure is used. The cylinder is loaded incrementally in five equal load steps. The following two material models are used:

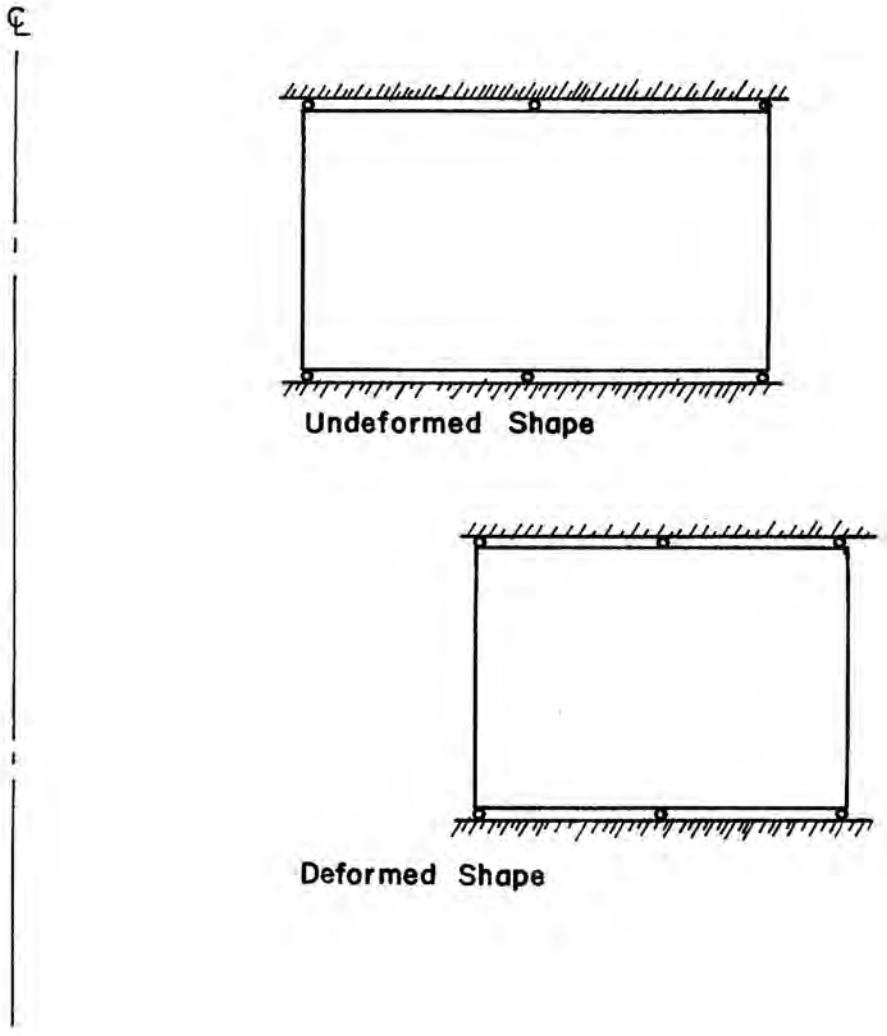

Fig. (4.2) One-element Axisymmetric Grid--
Undeformed and Deformed Shapes
(p=150 psi)

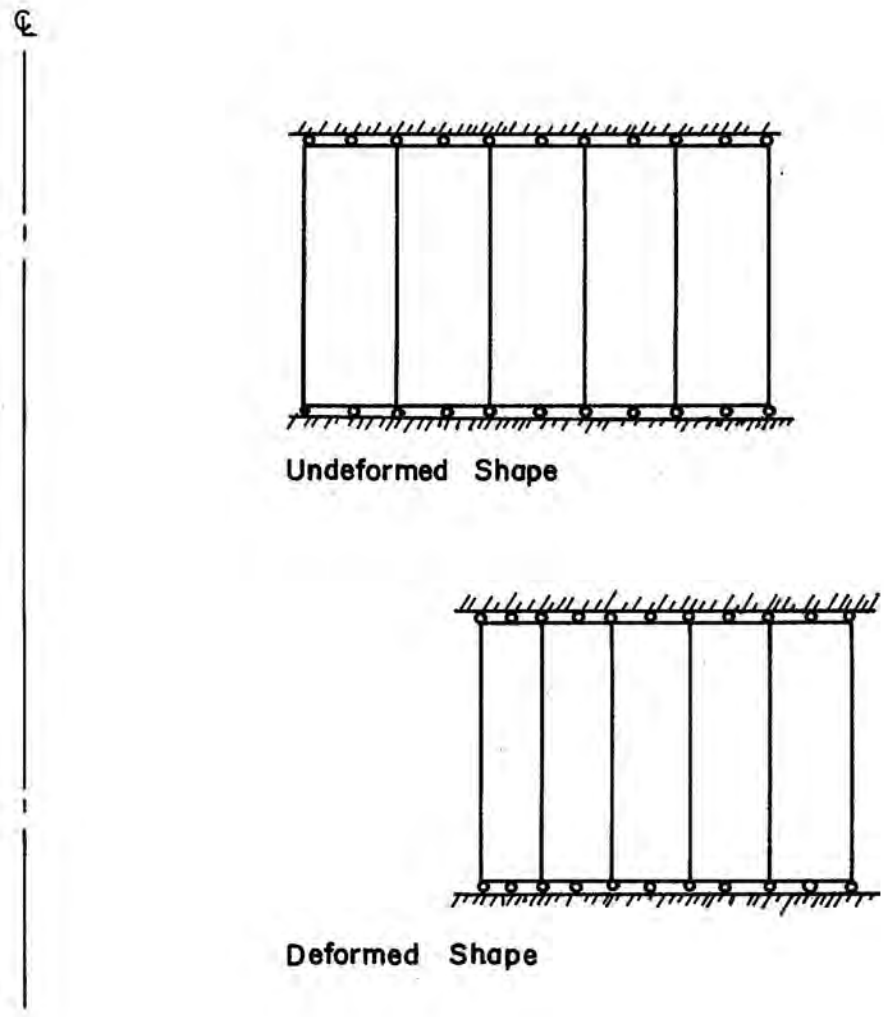

Fig. (4.3) Five-elemement Axisymmetric Grid--
Undeformed and Deformed Shapes
(p=150 psi)

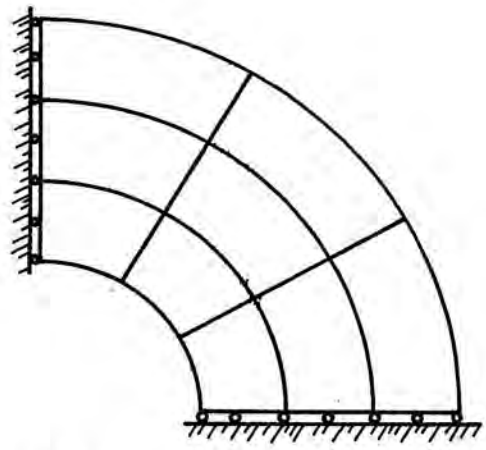

Undeformed Shape

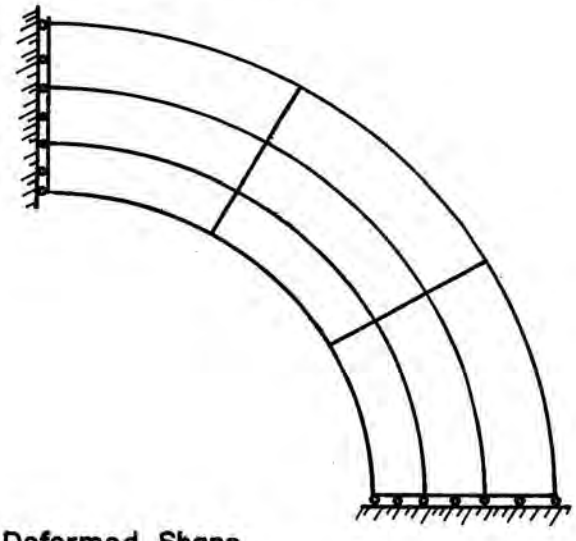

Deformed Shape

Fig. (4.4) Plane Strain Grid--Undeformed and Deformed Shapes (p=150 psi)

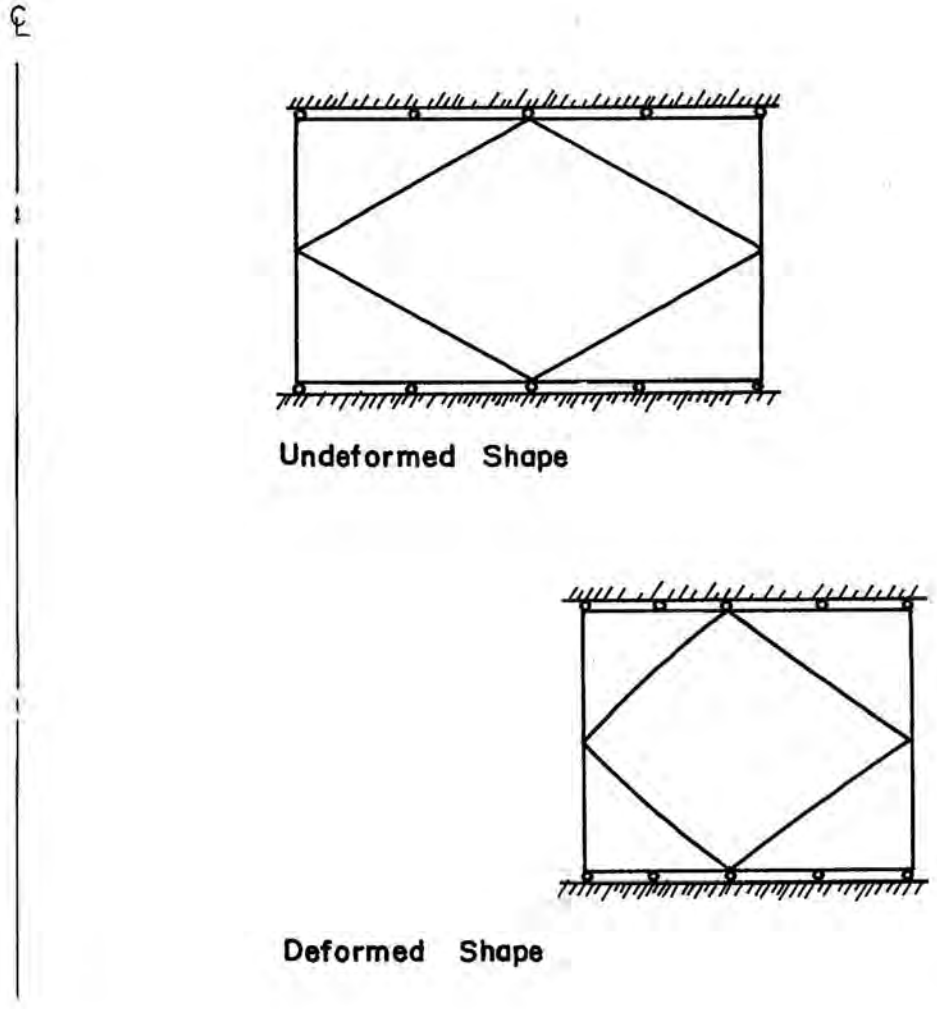

Fig. (4.5) Five-elemement Irregular Grid--
Undeformed and Deformed Shapes
(p=150 psi)

$$U = c_1(I_1 - 3) + c_2(I_2 - 3) + \lambda(\sqrt{I_3} - 1) \qquad (4.1)$$

$$U = c_1(I_1 - I_3 - 2) + c_2(I_2 - 2I_3 - 1)$$

$$+ R(\sqrt{I_3} - 1)^2 + \lambda(\sqrt{I_3} - 1). \qquad (4.2)$$

The results of the two mixed material models were identical; however the second model (with $R = 2(c_1 + c_2)$) converged a little (5%) faster than the first one. The second material model, though, is used for the rest of the applications, unless otherwise stated. A plot of the internal pressure (p) versus the radial displacement (u_r) of an interior node (with original radius = 7") is shown in Fig. (4.6). The stresses (radial σ_r and tangential σ_θ) calculated at the (2 × 2) Gauss integration points, are shown in Fig. (4.7). Fig. (4.6) and Fig. (4.7) show that the finite element solution is accurate; in fact, indistinguishable from the exact solution.

4.1.4 Comparison with Previous Solutions

Here we use three grids: a five-element axisymmetric grid, a one-element axisymmetric grid, and a nine-element plane strain grid. In all the grids nine-point integration rule is used.

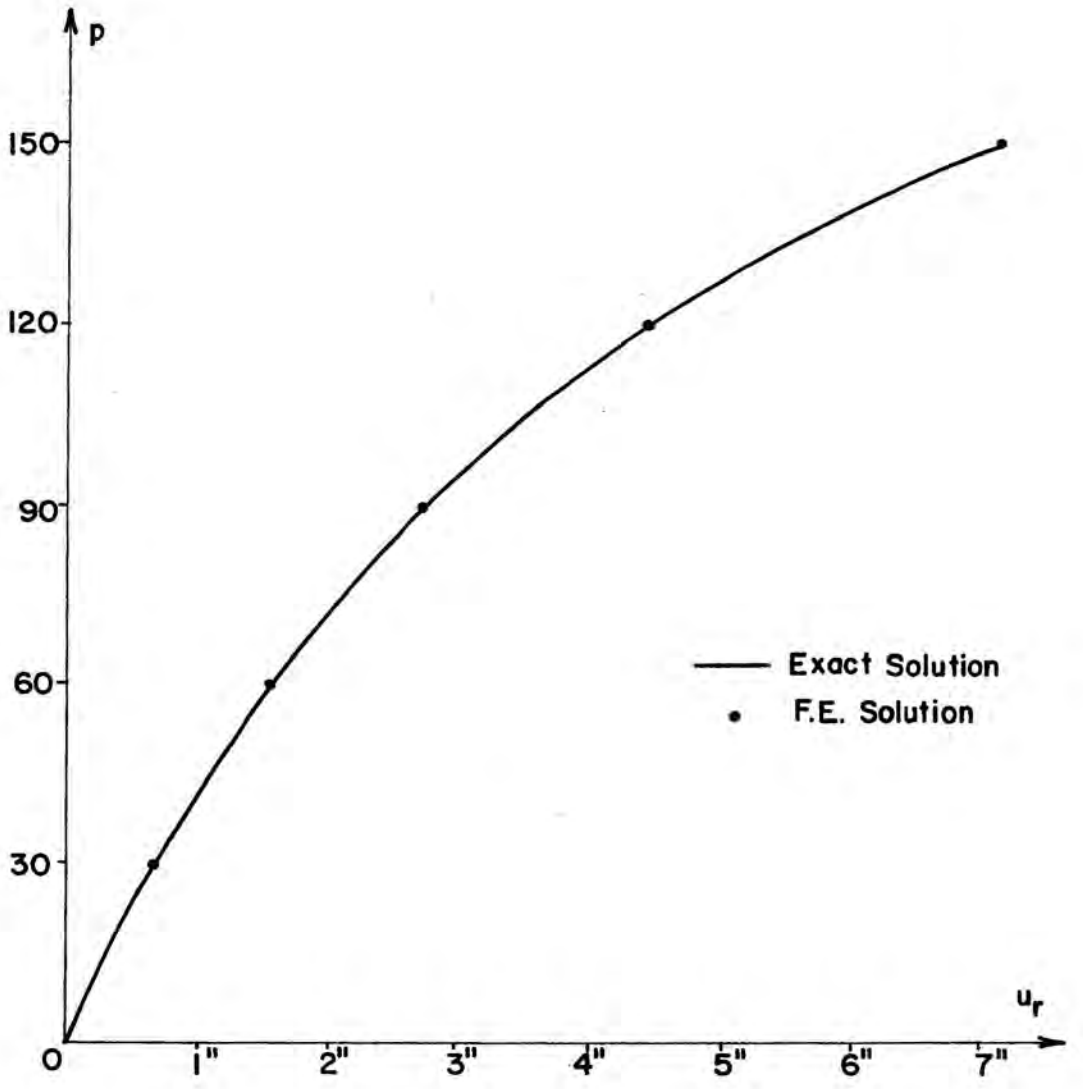

Fig. (4.6) The Pressure "p" vs. the Interior Nodal Displacement "u_r"

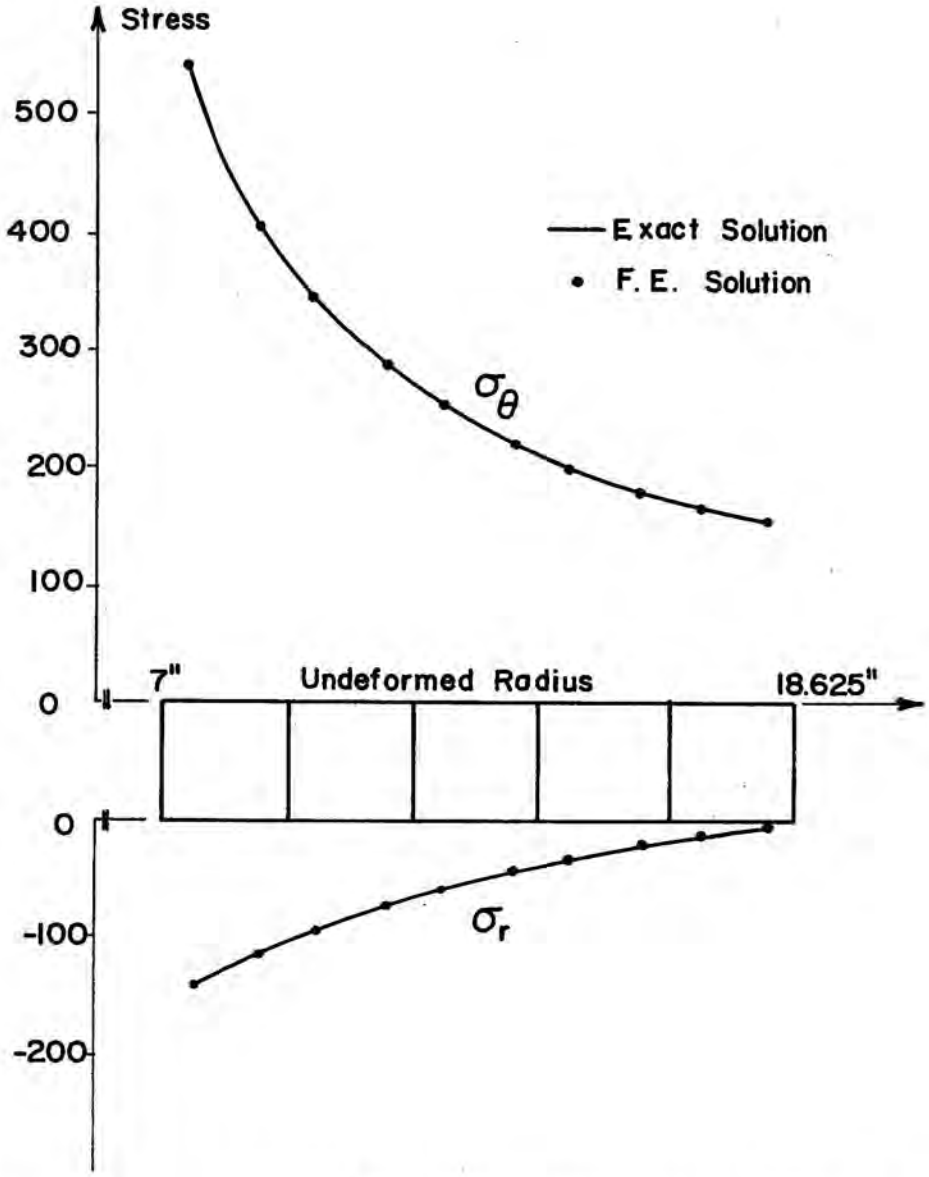

Fig. (4.7) Radial (σ_r) and Tangential (σ_θ) Stress Distributions (p=150 psi)

Oden and Key showed the effect of the number of elements on the accuracy of the solution. The number of elements across the thickness varies from one to nine, Fig. (4.8a). In the same figure we also plot our results (PR). It is clear that our one quadratic element gives results of superior accuracy compared to the linear element results of Oden and Key.

Scharnhorst and Pian showed the effect of the number of load increments on the accuracy of the solution. The number of load steps varies from 3 to 57, Fig. (4.8b). The figure also shows our present results (PR) using the five-element grid. We applied the pressure in one load step, and iterated to equilibrium. This looks more convenient than applying the pressure in many steps without using equilibrium iterations, since with five equilibrium iterations we obtained better results than the 57 load-increment results of Scharnhorst and Pian [27].

In Table (4.1) we compare our results (radial displacement u_r, radial stress T_{rr}, radial strain E_{rr}, tangential stress $T_{\theta\theta}$ and tangential strain $E_{\theta\theta}$) to the results obtained by Batra [2]. The comparison shows that our results are both more accurate and more efficiently obtained.

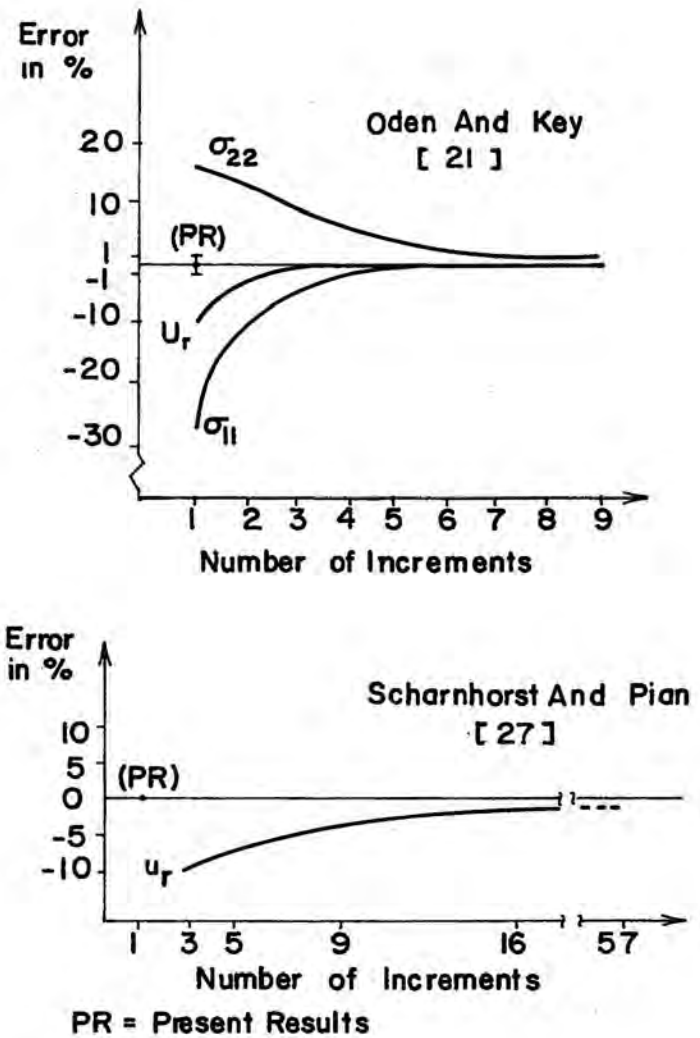

(Fig. 4.8) Comparison with Previous Results Reported in Refs. [21] and [27]

TABLE 4.1

BATRA'S RESULTS VS. THE PRESENT RESULTS

Results	No. of load inc.	u_r	$E^+_{\theta\theta}$	E^+_{rr}	$T^+_{\theta\theta}$	T^+_{rr}
Batra's Analysis Ref. [2]	50 load inc. with up to 15 eq. iter.	7.152	1.317	-.365	539	-134
	Exact	7.182	1.323	-.363	539	-135
	% Error	.4	.45	-.55	0	-.74
Present Results [PR]	1 load inc. with up to 5eq. iter.	7.182	1.355	-.365	551.1	-137.4
	Exact	7.182	1.356	-.365	550.9	-137.3
	% Error	0	.07	0	-.02	-.07

$^+$Evaluated at the Centroid for Ref. [2] and at the Inmost Integration Point for [PR].

The reason for the better accuracy we obtained is the fact that we did not introduce any approximation or simplification in our tangent matrix formulation; while the other investigators did.

The reason for the better efficiency we obtained is the fact that we included a load matrix, which is essential for problems of this type with the load being dependent on the deformations.

The importance of the load stiffness matrix is illustrated in Table (4.2). The pressure is allowed to increase gradually beyond the 150 psi; and both the axisymmetric five-element grid (AXI) and the plane strain nine-element grid (PLS) are used. In each case the solution is obtained with the presence (LS) and absence (NLS) of the load matrix. The number of iterations (N) when the load matrix was not included was at least five times higher than the number of iterations when the load matrix was there. This, no doubt, explains the very slow convergence in the work of Batra [2] and Skala [29]. The pressure (p) versus the interior nodal displacement (u_r), given in Fig. (4.9), indicates that there is a limit pressure, and this limit is around 200 psi. The theoretical results, given in Table (4.3), indicate that the cylinder would expand without limit had the pressure reached 200 psi.

TABLE (4.2)

EFFECT OF LOAD STIFFNESS

p			150	165	180	187.5	195
AXI.	LS	u_r	7.182	9.571	14.02	18.92	44.78
		N	5	4	5	4	6
	NLS	u_r	7.182	9.571	14.02	-	-
		N	25	30	50	>60	>60
PLS.	LS	u_r	7.182	9.571	14.02	18.92	44.78
		N	5	4	5	4	6
	NLS	u_r	7.182	9.571	-	-	-
		N	25	30	>60	>60	>60

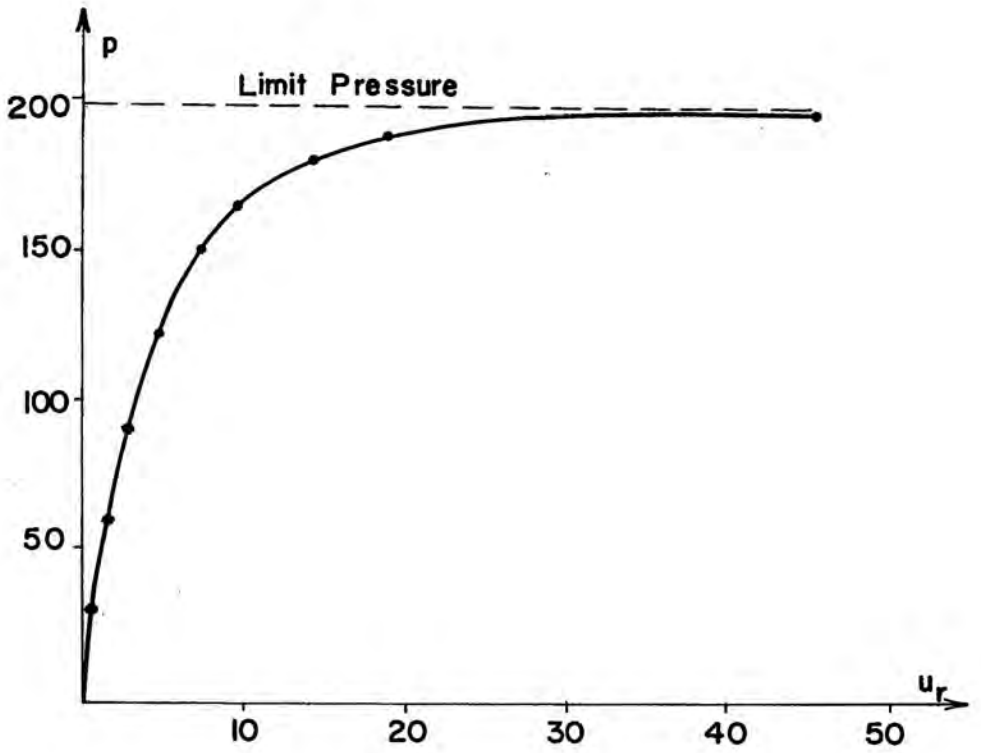

Fig. (4.9) The Pressure (p) vs. the Interior Nodal Displacement (u_r)

TABLE (4.3)

PRESSURE (p) VS. RADIAL DISPLACEMENT (u_r),

Ref. [8]

u_r	30	100	1000	10,000
p	193.26	195.67	195.72	196.72

4.1.5 Comparison between Mixed and Displacement Models

Here we use both the axisymmetric one-element grid and a plane strain grid with nine Serendipity elements. A nine-point integration rule is used, except for the penalty function term which is integrated using a four-point integration rule. The energy form for the displacement model is

$$U = c_1(I_1 - I_2 - 2) + c_2(I_2 - 2I_3 - 1) + \frac{1}{\varepsilon}(\sqrt{I_3} - 1)^2 \tag{4.3}$$

where

$$c_1 = 80 \text{ and } c_2 = 20.$$

If we view the penalized displacement calculations as a model for (slightly) compressible materials, it is interesting to know its initial shear and bulk modulii. For the strain energy used (Eq. (4.3)) the shear modulus (μ) is [5,6]

$$\mu = 2(c_1 + c_2). \tag{4.4}$$

The bulk modulus (K_o) is (see the appendix)

$$K_o = \frac{2}{\varepsilon} + \frac{4}{3}\,(2(c_1 - c_2)) \,. \qquad (4.5a)$$

And if $(1/\varepsilon)$ is large compared to c_1 and c_2 then the bulk modulus is approximated by

$$K_o = \frac{2}{\varepsilon} \,. \qquad (4.5b)$$

For the solution of nonlinear equations using the Newton method, a convergence tolerance (Tol.) needs to be specified. In our analysis we require

$$\frac{|\Delta u_i|}{|u_i|} \leq \text{Tol.}$$

and i runs from one to the total number of degrees of freedom.

In the displacement model, the incompressibility is satisfied using the penalty method, in which we specify a penalty parameter $(1/\varepsilon)$.

Fig. (4.10a) shows the absolute error, $|e|$, in the radial displacement versus a relative penalty parameter $(1/\varepsilon^*)$ which is given by

$$\frac{1}{\varepsilon^*} = \frac{1}{(c_1 + c_2)\varepsilon} \quad .$$

Actually $1/\varepsilon^*$ represents (equation (4.4) and (4.5b)) the ratio of bulk to shear modulii. Fig. (4.10b) shows the number of iterations (N) versus $(1/\varepsilon^*)$.

The two figures show that small ($< 10^2$) value of the penalty parameter $(1/\varepsilon^*)$ gives inaccurate results, while excessively large value ($> 10^5$) may prevent obtaining convergence with necessary precision (small tolerance).

Tables (4.4) and (4.5) show the convergence of the displacement model solution to the mixed model solution for both the axisymmetric and plane strain grids, respectively. In these tables the convergence tolerance (Tol) equals to 10^{-5}.

It is apparent from the data in Table (4.5) that the interior nodal displacement (u_r), the radial stress (σ_r) and tangential stress (σ_θ) converge to the corresponding mixed model results as $(1/\varepsilon)$ increases. But the number of convergence iterations (N) in the mixed model (N=5) is less than the number obtained when the displacement model is used. It is clear that the penalty function term introduces "very ill-conditioned matrices" [24] as $1/\varepsilon$ gets larger.

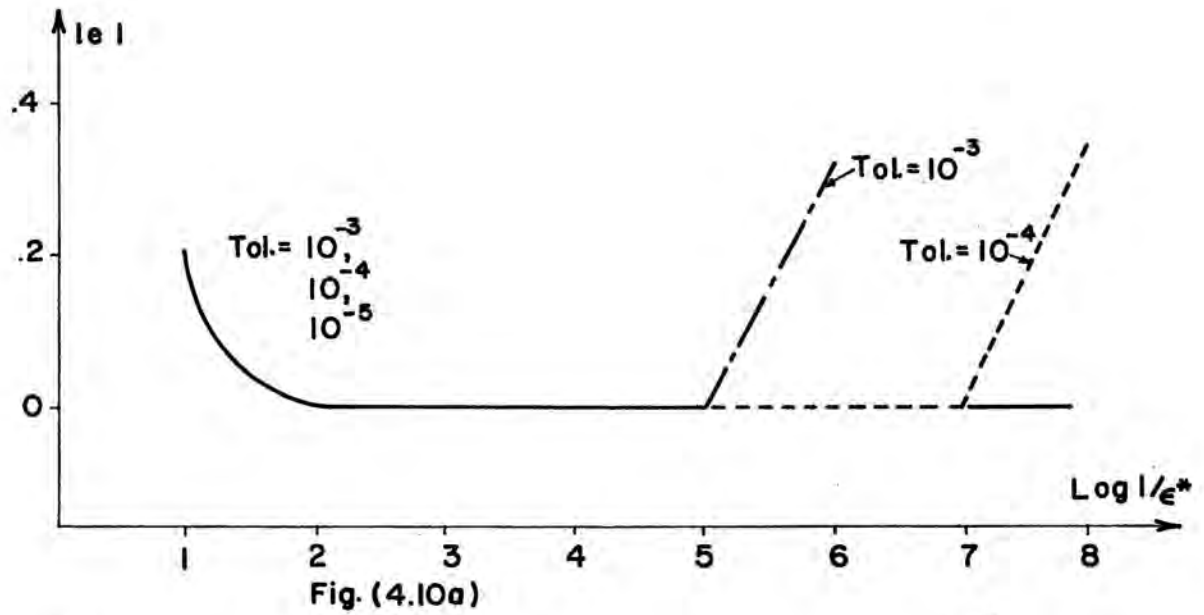

Fig. (4.10a)

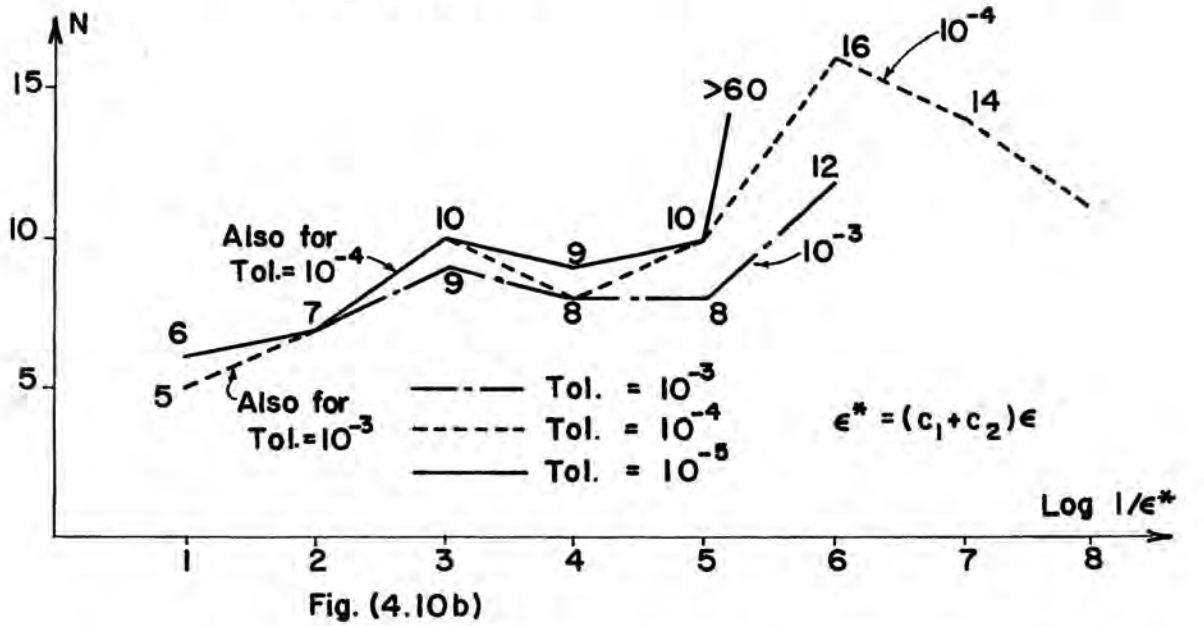

Fig. (4.10b)

Fig. (4.10) The Behavior of the Displacement Model (One-element Axisymmetric Grid)

TABLE (4.4)

MIXED AND DISPLACEMENT (ONE ELEMENT) MODELS

(AXISYMMETRIC CASE)

Model	$1/\epsilon^*$	N	u_r	σ_r	σ_θ
The Disp. Model	10^1	6	7.389	-95.82	379.6
	10^2	7	7.194	-95.91	374.2
	10^3	10	7.181	-95.92	373.7
	10^4	9	7.180	-95.92	373.6
	10^5	10	7.179	-95.95	373.6
	10^6	>60	-	-	-
The Mixed Model		5	7.176	-96.36	372.3
Exact			7.182	-95.50	370.7

TABLE (4.5)

MIXED AND DISPLACEMENT MODELS

(PLANE STRAIN CASE)

Model	$1/\epsilon^x$	N	u_r	σ_r	σ_θ
The Disp. Model	10^1	6	7.392	-1.29.4	526.4
	10^2	7	7.202	-129.5	512.6
	10^3	10	7.184	-129.5	511.2
	10^4	11	7.183	-129.5	511.1
	10^5	11	7.182	-129.5	511.1
	10^6	11	7.182	-129.5	511.1
	10^7	15	7.182	-129.5	511.1
	10^8	>40	-	-	-
The Mixed Model		5	7.182	-129.5	511.4
Exact			7.182	-129.5	511.0

4.1.6 Comparison between the Serendipity and Lagrangian Elements

The mixed model solutions of the one-and five-element grids are compared, when the following four elements were used:

1. Lagrangian element with conforming pressure (LC)
2. Lagrangian element with nonconforming pressure (LN).
3. Serendipity element with conforming pressure (SC)
4. Serendipity element with nonconforming pressure (SN).

The comparison is shown in Table (4.6), from which we conclude:

1. The Serendipity element is as accurate as the Lagrangian element, and is more efficient.
2. The nonconforming element is as accurate as the conforming element, and is more efficient.

The comparison, although extremely limited, may recommend the nonconforming Serendipity element for the mixed formulation.

4.1.7 Effect of the Integration Rule

Two grids are examined: a plane strain grid with nine curved side elements, and an axisymmetric grid

TABLE (4.6)

THE SERENDIPITY ELEMENTS (S)
VS.
THE LAGRANGIAN ELEMENTS (L);
THE CONFORMING ELEMENTS (C)
VS.
THE NONCONFORMING ELEMENTS (N)

	The One-element Grid				The Five-element Grid			
	u_r	σ_r	σ_θ	T(sec)	u_r	σ_r	σ_θ	T(sec)
LC	7.176	-96.36	372.30	2.13	7.182	-137.4	551.1	7.52
LN	7.176	-96.36	372.30	2.06	7.182	-137.4	550.9	7.17
SC	7.176	-96.36	372.30	1.95	7.182	-137.4	551.1	6.62
SN	7.176	-96.36	372.30	1.80	7.182	-137.4	550.9	6.29
Exact	7.182	-95.50	370.62		7.182	-137.3	550.9	

consisting of four triangular elements and one quadrilateral element. For the quadrilateral elements both the four- and nine-point quadrature rules are used, while four- and seven-point integration rules are used for the triangular elements. Table (4.7) shows the comparison between the four-point and the higher (called nine in the table) integration rule. Generally speaking the four-point rule is almost as good as the nine-point integration rule. The accuracy of the four-point rule was (1% at most) less than the accuracy of the other integration rule; however the efficiency was almost 50 percent higher with the four-point rule.

4.2 Compression of a Nonuniform Block

4.2.1 Problem Description

The problem considered here is concerned with the compression of a nonuniform prismatic plane strain block. This problem is a simplified version of a three-dimensional body tested at the Jet Propulsion Laboratory (JPL) of California Institute of Technology. A sectional plan at the middle surface of the test piece is shown in Fig. (4.11). A quarter cross section, which shows the

TABLE 4.7

THE NINE-POINT INTEGRATION (9-INT.) RULE VS. THE FOUR-POINT INTEGRATION (4-INT.) RULE

		9-INT	4-INT	EXACT
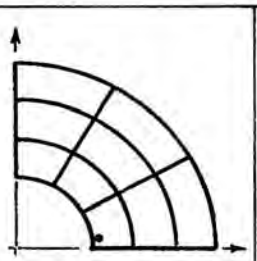 r = 7.769"	N	5	5	-
	T(sec)	8.38	4.68	-
	u_r	7.182	7.188	7.182
	σ_r	-129.5	-129.7	-129.46
	σ_θ	511.4	511.7	511.03
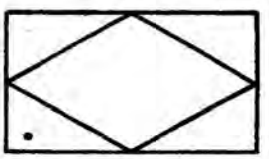 r = 8.938"	N	6	6	-
	T(sec)	4.98	2.95	-
	u_r	7.181	7.196	7.182
	σ_r	-100.8	-100.9	-105.4
	σ_θ	408.9	409.2	406.9

dimensions and boundary conditions, is shown in Fig. (4.12). The block was subjected to compression through the motion of the upper surface toward the lower surface. Both the upper and lower surfaces were perfectly bonded to rigid supports. A sketch of the experimental profiles is shown in Fig. (4.13). It is obvious from the sketch that the body exhibits cups located at .15 H from the upper and lower surfaces, with (H) being the total height of the block.

4.2.2 The Finite Element Solution

4.2.2.1 The Discretization Model. The finite element grid used for the solution of the problem is shown in Fig. (4.14). It consists of 45 elements, arranged five in the horizontal direction and nine in the vertical direction. The grid provides the following data

Number of displacement degrees of freedom	328
Number of constraint degrees of freedom	50
Net number of degrees of freedom	
328 - 50 =	278

With a nine-point integration rule:

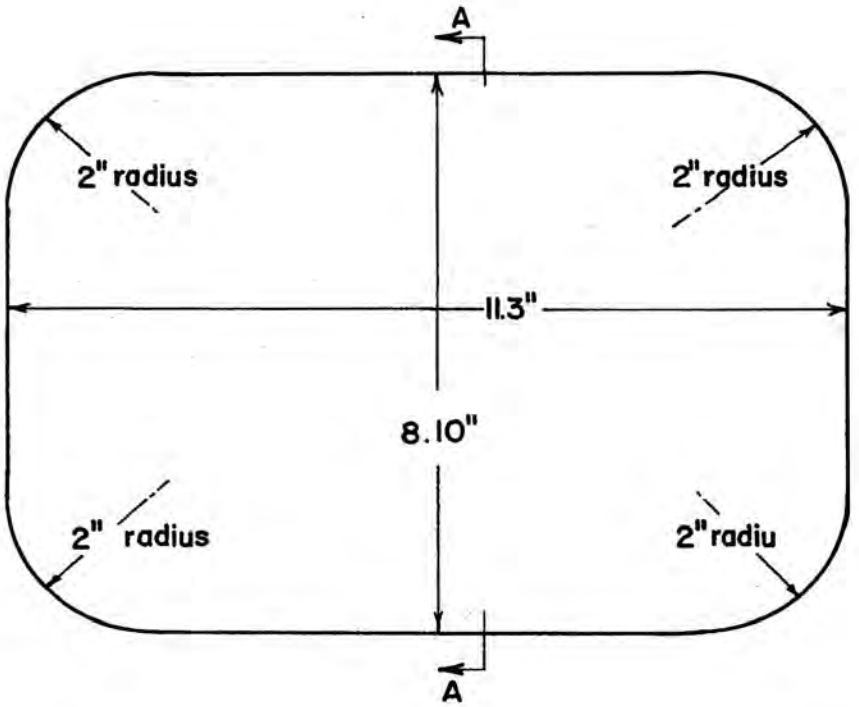

Fig. (4.11) Nonuniform Block--Center Plane at Zero Compressive Load

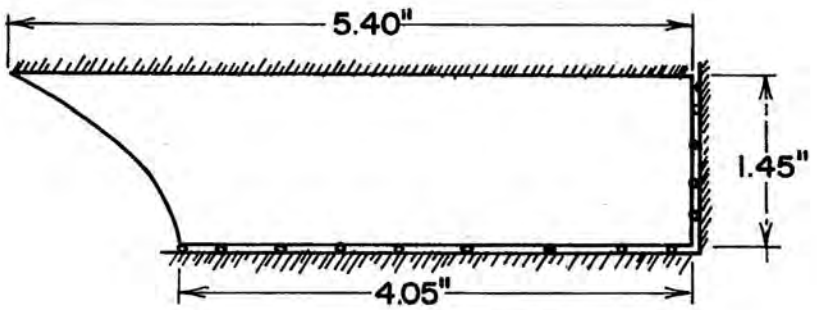

Fig. (4.12) Sec. A-A, of Fig. (4.11)

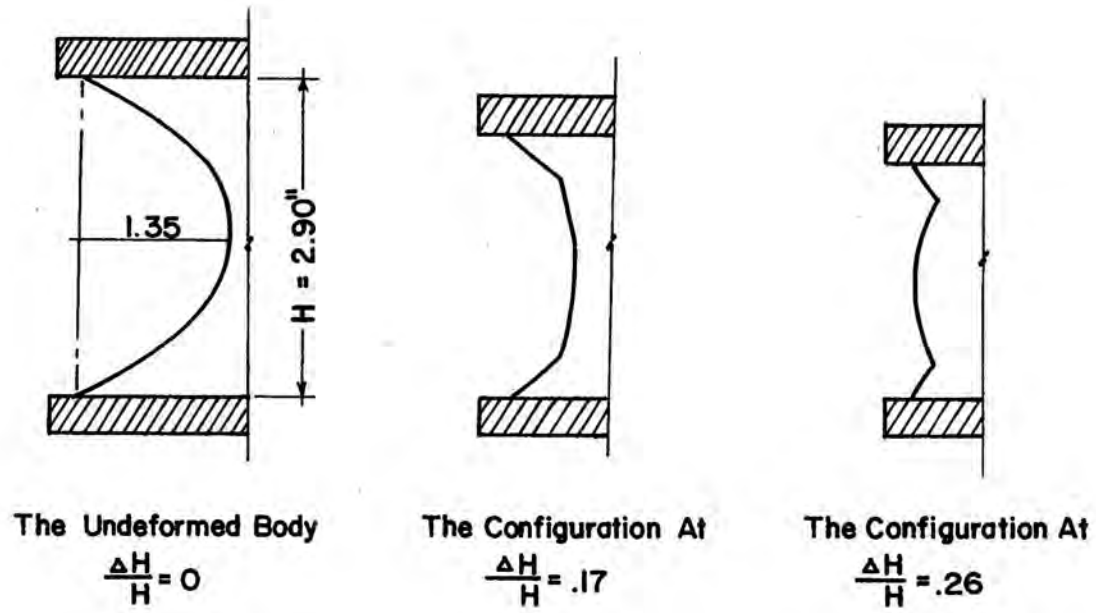

Fig. (4.13) Experimental Results Performed by the JPL Laboratory (3-D Model)

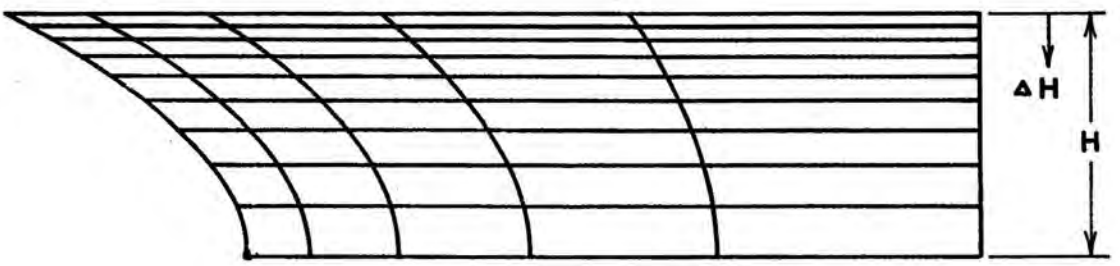

Fig. (4.14) The Finite Element Grid

Total number of constraint equations = 9 × 45 = 405

With a four-point integration rule:

Total number of constraint equations = 4 × 45 = 180

4.2.2.2 Material Models. Two forms of the strain energy for an incompressible material are studied. These are

1. Mooney form

$$U = c_1(I_1 - 3) + c_2(I_2 - 3)$$

2. The Three-term form

$$U = c_1(I_1 - 3) + c_2(I_2 - 3) + c_3(I_1 - 3)^2$$

with

$$c_1 = 1 \qquad c_2 = .5 \qquad c_3 = .25.$$

4.2.2.3 Formulation Models. In each of the material models three different variants of the problem formulation were used:

1. Mixed model (multiplier method) in which the incompressibility is included in the variational formulation by means of Lagrange multiplier (the hydrostatic pressure). The term added to the potential energy functional in this case is $\lambda(\sqrt{I_3} - 1)$. The pressure was modeled by both conforming (bilinear continuous) basis and by nonconforming (linear discontinuous) basis functions. No discernible differences were observed between the behavior of conforming and nonconforming pressure.
2. Modified mixed model (Augmented Lagrangian method) in which the formulation of Case 1 is modified by the addition of a "regularizing" term which has the form $100(\sqrt{I_3} - 1)^2$, to the variational statement.
3. Displacement model (penalty method) in which the incompressibility constraint is enforced by the addition of a penalty function in the form

$$\frac{1}{\varepsilon} (\sqrt{I_3} - 1)^2.$$

In this formulation, a modification of the energy

forms which provides for admissible initial tangent stiffness calculations (initial tangent modulus [5, 15]) is used. The energy forms used in the displacement model have the following forms:

Mooney

$$U = c_1(I_1 - I_3 - 2) + c_2(I_2 - 2I_3 - 1) + \frac{1}{\varepsilon}(\sqrt{I_3} - 1)^2$$

The Three Term

$$U = c_1(I_1 - I_3 - 2) + c_2(I_2 - 2I_3 - 1) + c_3(I_1 - 3)^2 + \frac{1}{\varepsilon}(\sqrt{I_3} - 1)^2$$

where

$$c_1 = 1, \quad c_2 = .5, \quad c_3 = .25 \text{ and } \frac{1}{\varepsilon} = 1{,}000.$$

Thus with two material models, and three formulation methods for each material model, we have six formulations of the problem. Throughout we use eight-node Serendipity element and nine-point integration rule for all the terms

except the penalty term in the displacement model which is integrated by a four-point rule.

4.2.3 Results

The finite element results for the two material models, and the different formulation methods, are shown in Figs. (4.15) through (4.19). Comparing the finite element results to the experimental results we find:

1. Mooney material model is not as good as the Three-term material model, the latter being more compatible with the experimental results.
2. Both the multiplier and penalty-method results (with the Three-term form) show reasonable agreement with the experimental results. Indeed the penalty-method results are not volume preserving (gives 97% of the volume with $1/\varepsilon = 1{,}000$). With a larger penalty parameter ($1/\varepsilon = 10{,}000$) the convergence becomes extremely difficult. But the pattern of deformation of the two methods is similar, and shows a cusp located at .15 H. Then the numerical procedure fails to converge after the cusp forms.
3. The Augmented Lagrangian method resulted in a rather regular solution, which does not look accurately like the experimental results.

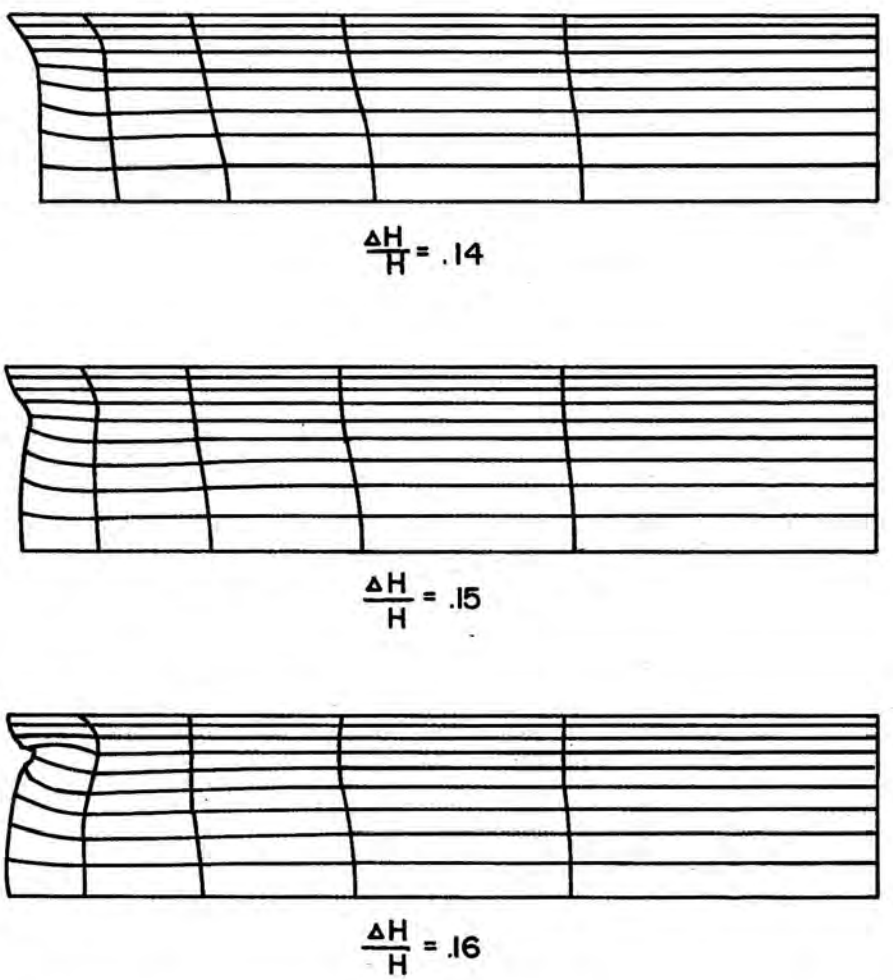

Fig. (4.15) Mooney Form--Multiplier Method

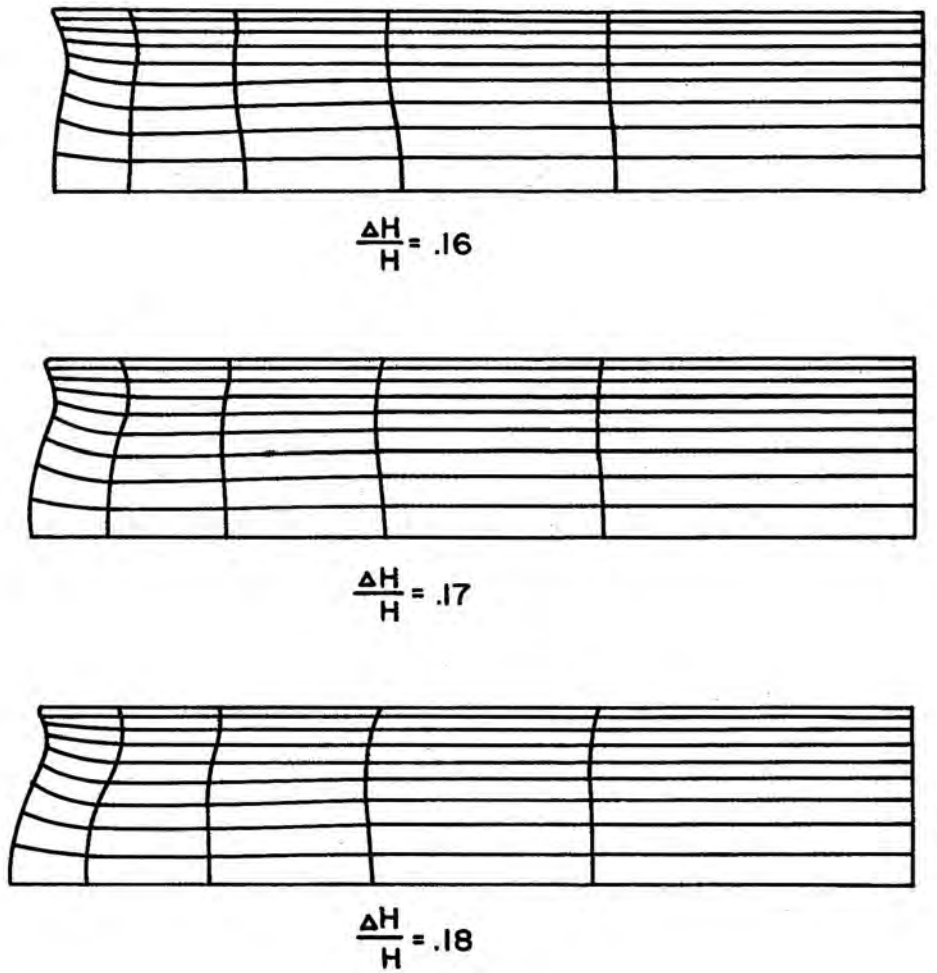

Fig. (4.16a) Modified Mooney form--Augmented Lagrangian Method ((ΔH/H) = .16, .17, .18)

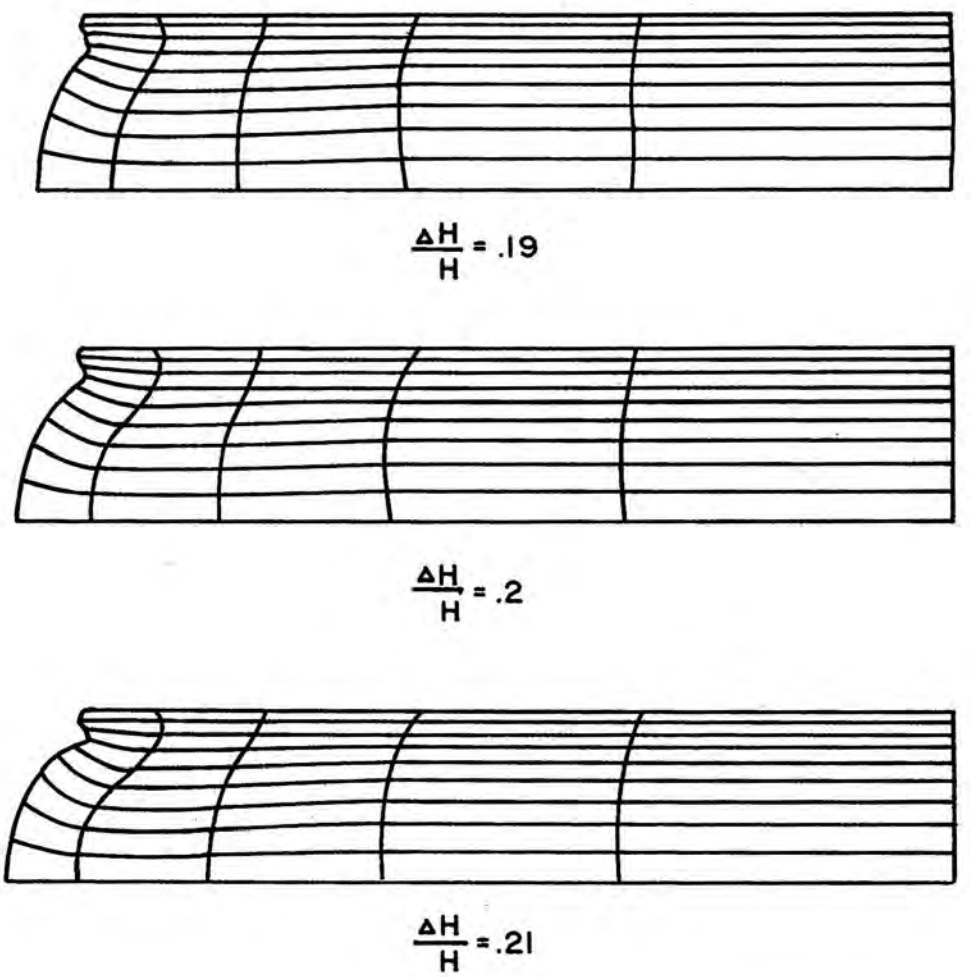

Fig. (4.16b) Modified Mooney Form--Augmented Lagrangian Method ($(\Delta H/H) = .19, .2, .21$)

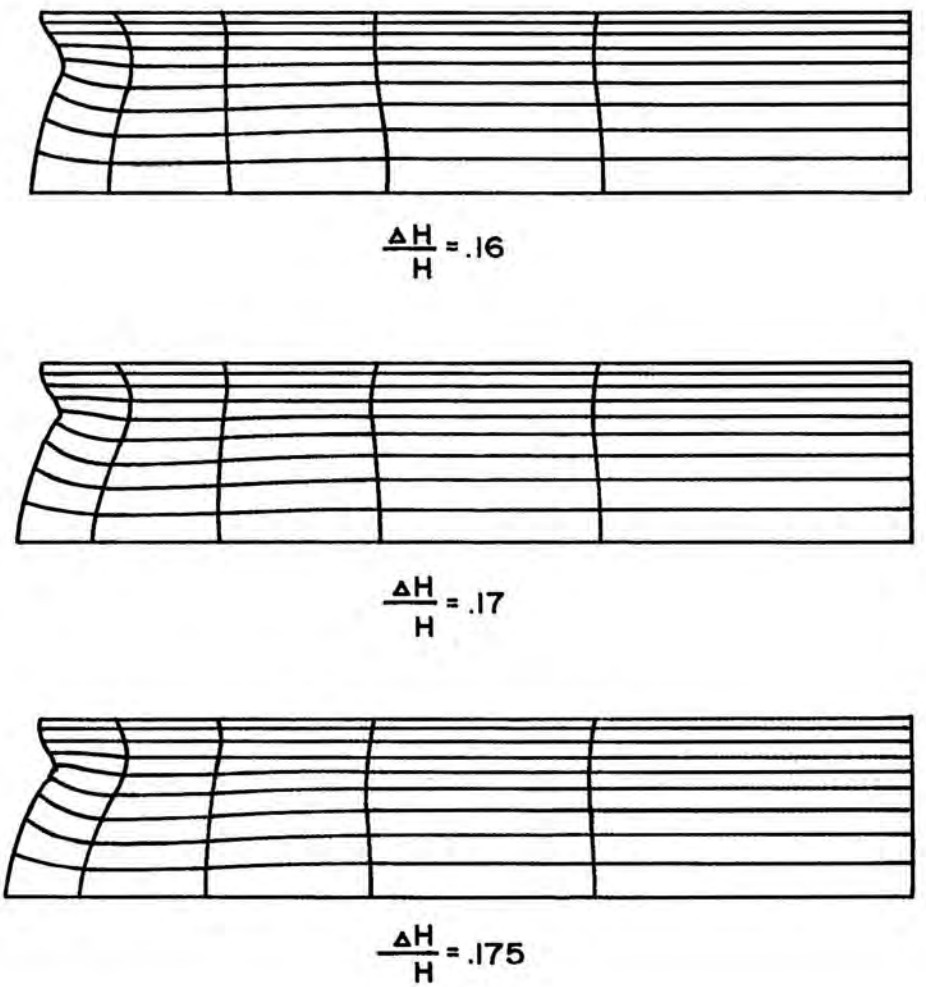

Fig. (4.17) Three-term Form--Multiplier Method

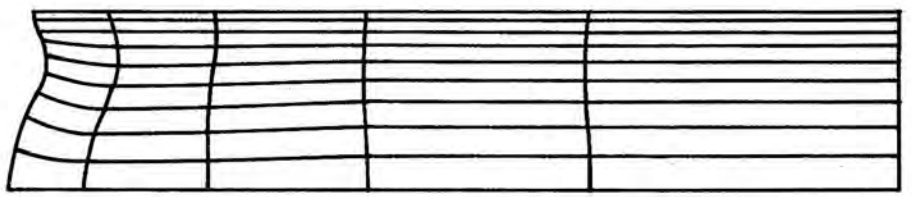

$\frac{\Delta H}{H} = .17$

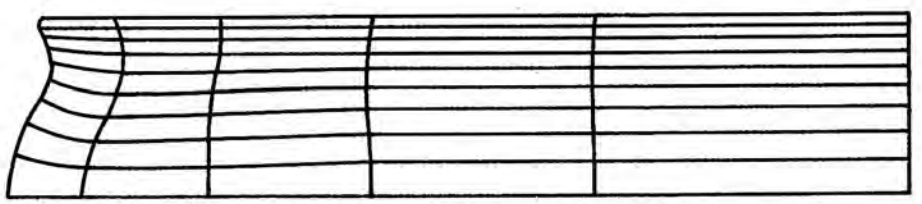

$\frac{\Delta H}{H} = .175$

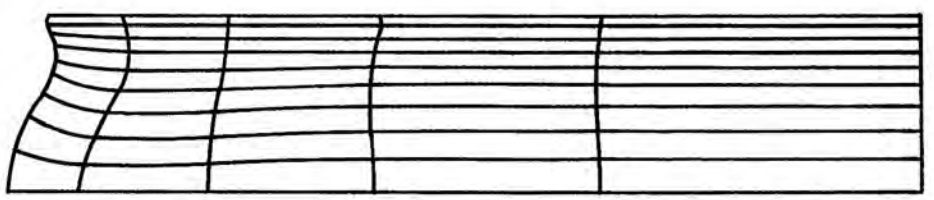

$\frac{\Delta H}{H} = .18$

Fig. (4.18a) Modified Three-term form--Augmented Lagrangian Method ($(\Delta H/H) = .17, .175, .18$)

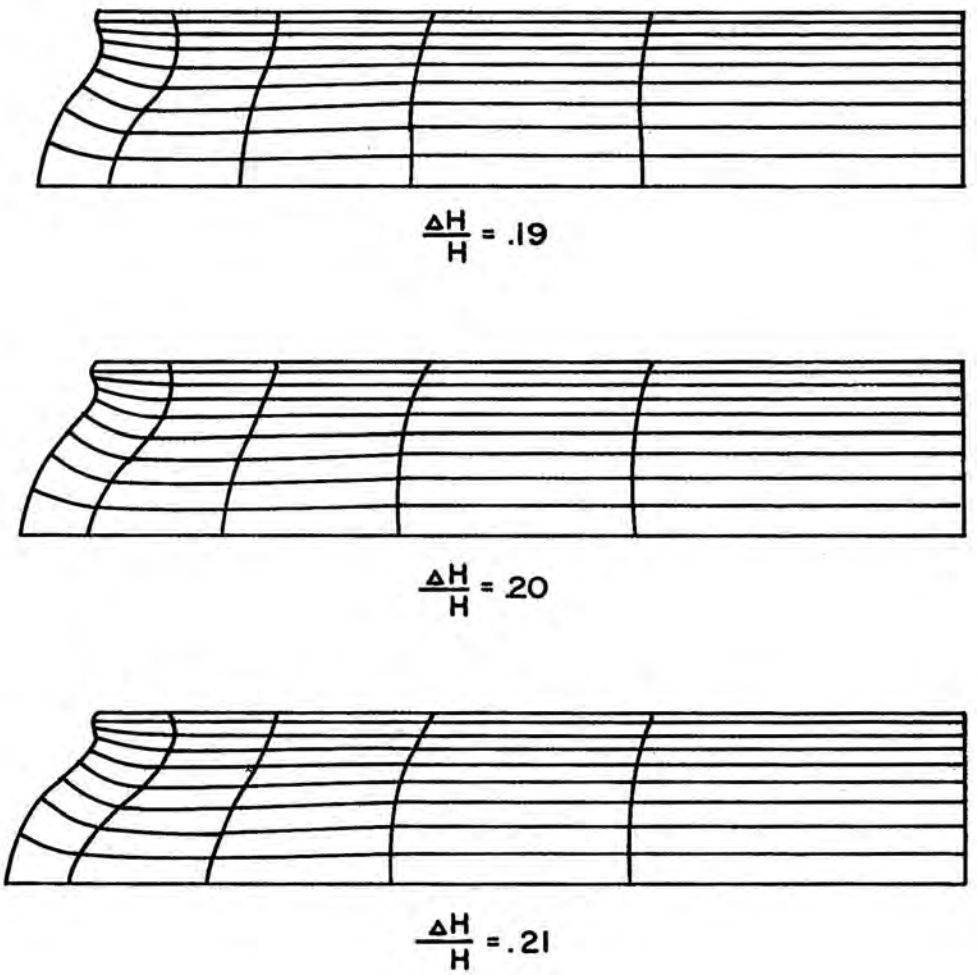

Fig. (4.18b) Modified Three-term form--Augmented Lagrangian Method ((ΔH/H) = .19, .2, .21)

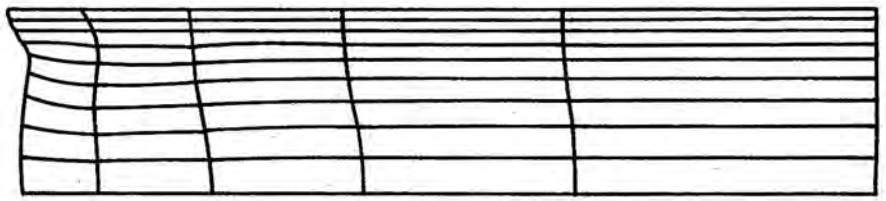

$\frac{\Delta H}{H}$ = .155-Mooney

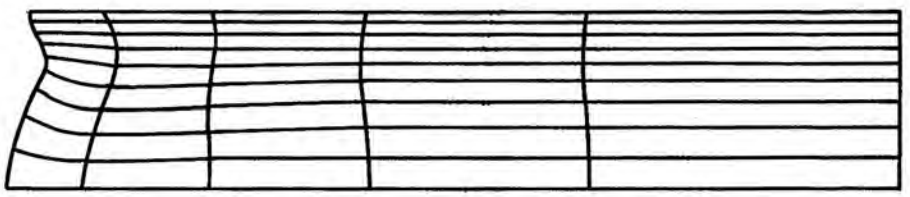

$\frac{\Delta H}{H}$ = .175 - 3T

Fig. (4.19) Mooney and Three-term (3T) Forms--
Displacement Models (Penalty Method)

4.2.4 Discussion of the Results

Here we try to answer one question, which is: Why does the Augmented Lagrangian method give a rather regular solution?

For this question we ran two sets of experiments. In the first set, the regularizing parameter (R) is allowed to vary. Fig. (4.20) shows the deformed shapes for three different values of (R). The results of this experiment show that the deformed shapes depend on the regularizing parameter. In the second experiment the integration rule changes from nine-point integration rule to four-point integration rule. The results of this experiment are shown in Fig. (4.21). Again the results of the four-point integration rule are different from the results obtained with the nine-point integration rule. The four-point rule produces deformed shapes that exhibit a cusp.

The last two experiments give one conclusion: it is that the mixed models can suffer "locking" the same way the displacement models (penalty method) do [34]. In other words, the regularizing term needs to be treated the same way a penalty term is treated; i.e., with a reduced integration. With the four-point integration rule, the

Augmented Lagrangian formulation gives consistent results with the previous results of the other two formulation methods.

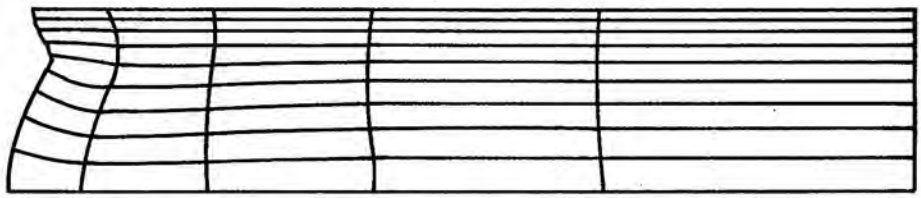

R = 3

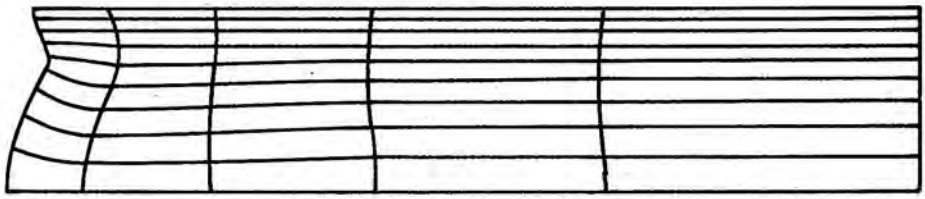

R = 10

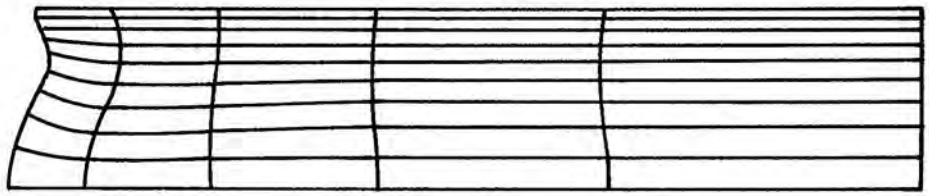

R = 100

Fig. (4.20) Three-term Form--Augmented Lagrangian Method--Nine-Point Integration Rule ($(\Delta H/H) = .17$)

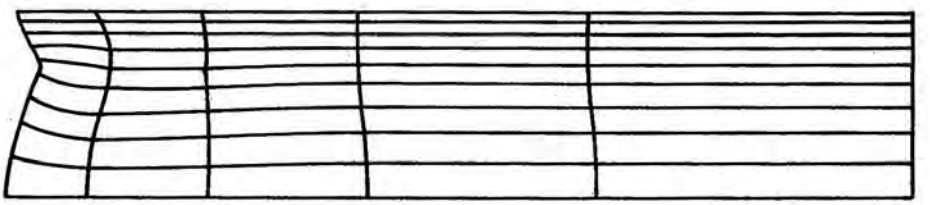

$\frac{\Delta H}{H} = .16$

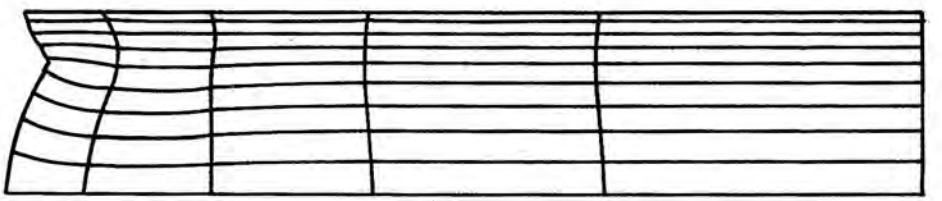

$\frac{\Delta H}{H} = .165$

Fig. (4.21) Three-term Form--Augmented Lagrangian Method--Four-point Integration Rule (R=100)

C H A P T E R V

SUMMARY OF RESULTS

5.1 Summary of Results

In this work, we give a finite element formulation method for the analysis of hyperelastic rubber-like materials, of a general isotropic constitutive law, subjected to the action of body forces and traction boundary conditions. The materials considered may be:

1. Compressible.
2. Nearly incompressible; in this case the energy form is augmented with (or includes) a penalty function (displacement model).
3. Incompressible; in this case the energy form is augmented with a multiplier function (mixed model). It is also possible here to add both a regularizing term (which looks like a penalty term but the regularizing parameter need not be very large), and the multiplier function. This formulation is called Augmented Lagrangian [24, 32].

Newton Raphson's method is used for solving the resulting nonlinear equilibrium equations. Tangent stiffness calculations cover the following cases:

1. Three-dimensional body
2. Plane strain body
3. Axisymmetric body

while load matrices are derived for the following cases:

1. Pressure loading acting on a plane strain body
2. Pressure loading acting on an axisymmetric body
3. Body force due to a rotation of an axisymmetric body about its centroidal axis.

Solutions are given for two problems: a pressurized thick cylinder and compression of nonuniform block. In the pressurized cylinder problem we showed that

1. The formulation of the finite element scheme presented is completely consistent with the virtual work equations. This consistency leads to improvements in accuracy and efficiency compared to typical results reported by others.
2. The addition of the load matrix resulted in reducing the number of iterations required to achieve convergence. When this matrix was neglected the number of iterations required was at least five times the number required when it was included.

3. The mixed models are preferable to the displacement models. In the latter models we must choose the value of the penalty parameter. This parameter affects the convergence of the iterative scheme. The penalty solution is shown to converge to the multiplier solution as the penalty parameter gets larger. A value of the penalty parameter equaling a thousand times the sum of the coefficients of the first and second strain invariants is recommended in the displacement models.
4. The eight-node Serendipity element is more efficient than the nine-node Lagrangian element, and in mixed models, an eight-node element with linear (nonconforming) pressure is shown to lead to an average saving in time of 6 percent over a corresponding eight-node element with bilinear (conforming) pressure.

For the compression of the nonuniform block two material models were tested: the Mooney form and the Three-term form. The behavior of every one of these forms was evaluated with and without a regularizing term. Comparing our results to the experimental results we observe the following:

1. The Three-term form is more compatible with the experimental results than the Mooney form. This is, of course, not always the case. Ref. [1] shows results of two tension tests performed on an 8 percent sulphur rubber, uniaxial and equibiaxial. Comparing the Three-term form to the Mooney form it was found that the Three-term form gives better correlation with the equibiaxial tension, but the uniaxial response obtained using the Mooney form was closer to the experimental results.
2. The regularizing term, in the mixed formulation (Augmented Lagrangian method), needs to be treated the same way as penalty function is treated, namely with reduced integration. Otherwise "locking" would occur.

5.2 Further Research

1. Special classes of displacement models based on the penalty method were introduced in Refs. [12, 16, 17]. A comparison between the mixed method solution as well as the convergence of the computation with these methods deserves further

research. Based on the results reported in these references we still suspect that the mixed method can do better than these methods.

2. We mentioned in Chapter III that the third strain invariant changes the calculated initial tangent when augmented with an energy form. In fact this may be useful in problems that have more than one solution. By changing the initial tangent (initial modulus of elasticity) we may be able to obtain the different solutions. One of the interesting problems would be the cube investigated by Rivlin [25, 26].

A P P E N D I X

1 Majerus Conditions

Majerus [15] set forth four conditions which restrict the possible choices for a strain energy function of compressible materials. These are:

$$(a)\left\{\left(\frac{\partial^2 U}{\partial I_1^2}+\frac{\partial^2 U}{\partial I_3^2}+2\,\frac{\partial^2 U}{\partial I_3^2}+2\,\frac{\partial^2 U}{\partial I_1\,\partial I_2}+2\,\frac{\partial^2 U}{\partial I_2\,\partial I_3}+\frac{\partial^2 U}{\partial I_1\,\partial I_3}\right)\right\}_0>0$$

$$(b)\left\{\frac{\partial U}{\partial I_2}+\frac{\partial U}{\partial I_3}\right\}_0<0$$

$$(c)\left\{2\,\frac{\partial U}{\partial I_2}+2\,\frac{\partial U}{\partial I_3}+3\,\frac{\partial^2 U}{\partial I_1^2}+12\,\frac{\partial^2 U}{\partial I_3^2}+3\,\frac{\partial^2 U}{\partial I_3^2}+12\,\frac{\partial^2 U}{\partial I_1\,\partial I_2}+6\,\frac{\partial^2 U}{\partial I_1\,\partial I_3}+12\,\frac{\partial^2 U}{\partial I_2\,\partial I_3}\right\}_0>0$$

$$(d)\left\{\frac{\partial U}{\partial I_1}+2\,\frac{\partial U}{\partial I_2}+\frac{\partial U}{\partial I_3}\right\}_0=0\,.$$

The four conditions apply at the stress-free $(.)_0$ state, for which $I_1 = I_2 = 3$ and $I_3 = 1$. The first three inequalities are restrictions on the strain energy to be positive definite. The last equation is simply a requirement that the unstrained body be still free.

2 Cheng's Formulas for the Initial "Young's" Modulus (E_0)

Cheng [5] derived the following formulas for the initial "Young's" Modulii, for both incompressible ($I_3 = 1$) and compressible ($U_{,1} + U_{,2} + U_{,3} = 0$) materials.

$$E_0^I = 6(U_{,1} + U_{,2})_0$$

$$E_0^C = [-3K_0(U_{,2} + U_{,3})]/[(U_{,2} + U_{,3})_0 + 2(U_{,11} + 4U_{,22} + U_{,33})_0 + 4(2U_{,33} + U_{,31} + 2U_{,12})_0]$$

and K_0 (the initial bulk modulus) is given by

$$K_0 = \frac{4}{3}[2(U_{,2} + U_{,3})_0 + 3(U_{,11} + 4U_{,22} + U_{,33})_0 + 6(2U_{,23} + U_{,31} + 2U_{,12})_0]$$

where

$$U_{,i} = \frac{\partial U}{\partial I_i} \quad , \quad U_{,ij} = \frac{\partial^2 U}{\partial I_i \, \partial I_j}$$

R E F E R E N C E S

R E F E R E N C E S

1. Alexander, H. "A Constituve Relation for Rubber-like Materials," Int. J. Engng. Sci. 6, 549-563 (1968).

2. Batra, R. C. "Finite Plane Strain Deformations of Rubber-like Materials," Short Communication, Inc. J. Num. Meth. Engng. 15, 145-160 (1980).

3. Becker, E. B. "A Numercial Solution of a Class of Problems of Finite Elastic Deformation," Ph.D. dissertation, University of California, Berkeley, 1966.

4. Becker, E. B., Carey, G. F. and Oden, J. T. Finite Elements: An Introduction, Vol. I, Prentice-Hall, Englewood-Cliffs, N.J. (1981).

5. Cheng, K. "Determination of a Strain Energy Function for Rubbers," Lord Report RD75-007 (1975).

6. Cescotto, S. and Fonder, G. "A Finite Element Approach for Large Strains of Nearly Incompressible Rubber-like Materials," Int. J. Solids Structures 15 589-605 (1979).

7. Fung, Y. C. "Foundation of Solid Mechanics," Prentice-Hall, Inc., Englewood Cliffs, N.J. (1965).

8. Green, A. E. and Zerna, W. Theoretical Elasticity, 2nd ed., Oxford University Press, London (1968).

9. Hibbitt, H. D., Marcal, P. V. and Rice, J. R. "A Finite Element Formulation for Problems of Large Strain and Large Displacement," Int. J. Solids Structures 6, 1069-1086 (1970).

10. Hibbitt, H. D. "Some Follower Forces and Load Stiffness," Int. J. Num. Meth. Engng. 14, 937-941 (1979).

11. Lee, D. C. Nonlinear Continuum Mechanics, McGraw-Hill, New York (1968).

12. Jankovich, E., Leblanc, F., Durand, M. and Bercovier, M. "A Finite Element Method for the Analysis of Rubber Parts, Experimental and Analytical Assessment," to appear.

13. Le Tallec, P. "Numerical Analysis of Equilibrium Problems in Incompressible Nonlinear Elasticity," Ph.D. dissertation, The University of Texas, Austin (1980).

14. Luenberger, D. G. Introduction to Linear and Nonlinear Programing, Addision Wesley, Reading, Mass. (1973).

15. Majerus, J. N. "Restrictive Conditions on Elastic Potential for a Compressible Anisotropic Hyperelastic Solid," Rohm Haas Technical Report S-225 (1970).

16. Malkus, D. S. and Hughes, R. J. R. "Mixed Finite Element Methods--Reduced and Selective Techniques: A Unification of Concepts," Comp. Meths. Appl. Mech. Eng. 15, 63-81 (1978).

17. Malkus, D. S. "Finite Elements with Penalties in Nonlinear Elasticity," Int. J. Num. Meth. Engng. 16, 121-136, 1980.

18. McMeeki, R. and Rice, J. R. "Finite Element Analysis for Problems of Large Elastic-Plastic Deformation," Int. J. Solids Structures 11, 606-616 (1975).

19. Nagtegaal, J. C., Parks, D. M. and Rice, J. B. "On Numerically Accurate Finite Element Solutions in the Folly Plastic Range," Comp. Meth. Appl. Mech. Engng. 4, 153-177 (1974).

20. Oden, J. T. Finite Elements of Nonlinear Continua, McGraw-Hill, New York (1970).

21. Oden, J. T. and Key, J. E. "Numerical Analysis of Finite Axisymmetric Deformations of Incompressible Elastic Solids of Revolution," Int. J. Solids Structures 6, 497-518 (1970).

22. Oden, J. T. and Kikuchi, N. "Existence Theory for a Class of Problems in Nonlinear Elasticity: Finite Plane Strains of Compressible Hyperelastic Body," TICOM Report, Austin, 1979.

23. Oden, J. T. and Le Tallec, P. "Compatibility Condition and Existence Results in Discrete Finite Incompressible Elasticity," to appear.

24. Powell, M. J. D. "Algorithm for Nonlinear Constraints that Use Lagrangian Functions," Mathematical Programing 14, 224-248 (1978).

25. Rivlin, R. S. "Large Elastic Deformations of Isotropic Materials II--Some Uniqueness Theorems for Pure Homogeneous Deformation," Phil. Trans. Roy. Soc. A, 491-508 (1948).

26. Rivlin, R. S. "Stability of Pure Homogeneous Deformation of of an Elastic Cube under Dead Loading," Q. A. M. 32, 265-271 (1974).

27. Scharnhorst, T. and Pian, H. H. "Finite Element Analysis of Rubber-like Materials by a Mixed Model," Int. J. Num. Meth. Engng. 12, 665-676 (1978).

28. Skala, D. P. "Large Strain Finite Element Analysis," Lord RD Report RD75-003 (1975).

29. Skala, D. P. "Large Strain Finite Element Analysis for a Compressible Elastic Material," Proc. Symp. Appl. Comp. Meth. Engng., Los Angeles, California (1977).

30. Stern, M. "An Approximate Shell Theory for Unrestricted Elastic Deformations," Int. J. Solids Structures 3, 905-927, 1967.

31. Stricklin, J. A., Riesemann, W. A., Tillerson, J. R. and Haisler, W. E., "Static Geometric and Material Nonlinear Analysis," Advances in Computational Methods in Structural Mechanics Design, University of Alabama Press, 301-324 (1972).

32. Tapia, R. A. "Augmented Lagrangian Methods for Constraint Optimization: The Role of the Penalty Constant," Presented at the International Conference on Nonlinear Optimization and Applications, L'Aquila, Italy, June 1979, also presented at UT Austin, 1980.

33. Yamada, Y. "Incremental Formulation for Problems with Geometric and Material Nonlinearities," Advances in Computational Methods in Structural Mechanics Design, University of Alabama Press, 325-335 (1972).

34. Zienkiewich, O. C. The Finite Element Method in Engineering Science, McGraw-Hill, London, 3rd ed. (1977).

Martha Ann Zirley typing service

2707 HEMPHILL PARK • AUSTIN, TEXAS 78705 • AC 512 472-3210

A FINITE ELEMENT ANALYSIS FOR PROBLEMS OF LARGE STRAIN AND LARGE DISPLACEMENT

Publication No. _____

Amin Saleh Aly, Ph.D.
The University of Texas at Austin, 1981

Supervising Professor: Eric B. Becker

The principle of virtual work, set in a Lagrangian frame of reference, is used for a finite element formulation of nonlinear boundary value problems for hyperelastic materials at large strains. The formulation is applicable to a general isotropic form of the strain energy function, and uses the Newton Raphson technique for incremental iterative analysis. In the discrete problem, two models are considered to simulate the behavior of rubber-like materials. The first model is a displacement model that has the displacement as the only variable. The second model is a mixed model that has both the displacement and hydrostatic pressure as variables. The performances of the eight-node Serendipity element and the nine-node Lagrangian element are discussed.

The formulation of the finite element scheme presented here is completely consistent with the virtual work equations. This consistency leads to good accuracy and rapid convergence of the computations.

TABLE OF CONTENTS

L I S T O F T A B L E S

L I S T O F F I G U R E S